

May 2026

**IEA Wind TCP Task 49**

**The IEA Wind RFA2  
Intermediate-Depth  
Reference Floating Array  
Design**



**Prepared for the  
IEA Wind TCP**



**May 2026**

**Authors:**

**Chris Wright, Dallán Friel, Ali Reza Vatandoust, Sahar Tavangar, James McAteer, Harrison Bishop, Mohammed Alaa Almoghayer, Louis-Marin Lapastoure, Emma Gallagher, Nishita Ravuri, Jean-Philippe Touzane**  
Gavin & Doherty Geosolutions, Venterra Group, Ireland

**Ju Feng**

DTU Technical University of Denmark

**Yong-Yook Kim**

Institute for Advanced Engineering, Korea

**Katherine Coughlan**

University College Cork, Ireland

**Mohammad Youssef Mahfouz**

University of Stuttgart, Germany

*IEA Wind TCP functions within a framework created by the International Energy Agency (IEA). Views, findings, and publications of IEA Wind do not necessarily represent the views or policies of the IEA Secretariat or of all its individual member countries. IEA Wind is part of IEA's Technology Collaboration Programme (TCP).*

## Version Control

Version No.	Date	Description	Prepared by	Checked by
0.1	24/04/2026	First draft circulated for IDEA internal review	CW, DF, ARV, ST, JM, HB, MAA, LML, EG, NR, JPT, JF, MYM, YYK, KC	GB
1.0	19/05/2026	Public Release	CW	KC

## Funding

GDG and UCC's involvement in the IDEA project is partially funded through SEAI's IDEA-IRL project under grant number 22/RDD/804.

## Acknowledgements

The authors would like to thank the support of the wider IEA Wind Task 49 Work Package 2 working group involved in the intermediate water depth reference farm design: Fiona Devoy McAuliffe, Milad Moghtadaei, Lars Frøyd, Madhan Mohan, Jiang Zhiyu, Xinyue Guo, Younglae You, H.P. Jostad, Muk Chen, Chern Fong, Yong-Yook Kim, Lin Li, Matt Hall and Erika Lozon.

## Executive Summary

This report provides a reference design for an intermediate-water-depth floating wind farm. The work was carried out under Task 49 of the International Energy Agency Wind Technology Collaboration Programme (IEA Wind TCP). The site is based on a generalized version of the Utsira Nord, Norway site with a water depth of 300 m.

To create a 1 GW farm, 67 units of the IEA Wind 15 MW reference wind turbine mounted on the steel VoltturnUS-S semi-submersible were selected.

A 3-line catenary mooring system, composed of wire rope in the water column and ground chain was selected for the design. An iterative design process involving integrated load assessment (ILA) led to the presented design, which includes a clump weight at the chain wire interface in order to maintain positive tensions at all times. The mooring design passes ultimate and fatigue limit state checks.

A lazy-wave dynamic cable configuration was designed using a decoupled analysis procedure. Outputs from the integrated load assessment (ILA), specifically the semi-submersible motions, were used as inputs to improve computational efficiency.

An investigation of annual energy production considering different site boundaries was conducted. Uniform vs non-uniform mooring headings for the array layout were also investigated. Inter-array cabling (IAC) was designed, considering seven strings of cables connected to a single offshore substation (OSS).

The baseline floating wind reference farm presented in this report was designed for use by the floating wind community as a common framework for future studies. Publicly available input files of load case tables, simulation files as well as the array ontology definition are available at the IEA Wind Task 49 GitHub website

## Table of Contents

<b>Acknowledgements</b> .....	<b>2</b>
<b>Executive Summary</b> .....	<b>3</b>
<b>Table of Contents</b> .....	<b>1</b>
<b>List of Figures</b> .....	<b>2</b>
<b>List of Tables</b> .....	<b>3</b>
<b>List of Acronyms</b> .....	<b>4</b>
<b>1 Introduction</b> .....	<b>5</b>
1.1 VoltturnUS-S semi-submersible platform .....	5
1.1.1 Hydrodynamic properties .....	5
1.1.2 WTG Controller.....	6
<b>2 Site Conditions</b> .....	<b>6</b>
2.1 Metocean Conditions .....	6
2.2 Ground Conditions.....	8
2.3 Design Load Case .....	8
2.3.1 Fatigue binning .....	10
<b>3 Mooring Design</b> .....	<b>11</b>
3.1 Simulation.....	12
3.2 Design Criteria.....	12
3.3 Description of Mooring System.....	12
3.4 Mooring ULS Results .....	15
3.5 Mooring FLS Results.....	15
<b>4 Anchor Design</b> .....	<b>18</b>
4.1 Methodology.....	18
4.2 Loading.....	18
4.3 Sizing 18	
<b>5 Dynamic Cable Design</b> .....	<b>20</b>
5.1 Overview.....	20
5.2 Design Procedure.....	20
5.3 Initial Design .....	20
5.4 Basic Design .....	21
5.5 Design Conditions.....	21
5.6 Design Criteria.....	21
5.7 Description of the Dynamic Cable System.....	22
5.7.1 Cable.....	23
5.7.2 Bend Stiffener.....	24
5.7.3 Buoyancy Modules .....	25
5.8 Dynamic cable analysis results .....	25
<b>6 Array Design</b> .....	<b>27</b>
6.1 Annual Energy Production (AEP) .....	27
6.2 Layout Optimization.....	28
6.3 Optimization of mooring system headings .....	29
6.4 Inter-Array Cabling (IAC).....	31
<b>7 Conclusions</b> .....	<b>35</b>
<b>References</b> .....	<b>36</b>
<b>Appendix A. Fatigue Binning Representability</b> .....	<b>37</b>

## List of Figures

Figure 1-1: The Norwegian economic zone with proposed offshore wind farm projects (left) and the Utsira Nord site (right) .....	6
Figure 1-2: Metocean data: (a) Mean wind speed at height 150 m, (b) Significant wave height $H_s$ , (c) Spectral Peak Period $T_p$ and (d) Current velocity at 0 m depth .....	7
Figure 1-3: Kernel density plots of Wave Significant height ( $H_s$ ) and (a) Wind speed, (b) Wind-wave misalignment and (c) Peak Period ( $T_p$ ).....	10
Figure 1-4: Rose plot of the Wave Energy by Wave direction.....	11
Figure 3-1: Description of mooring system.....	13
Figure 3-2: Mooring system headings at 0' (left) and 10' (right).....	16
Figure 3-3: Lifetime fatigue damage at all possible mooring headings .....	17
Figure 5-1: Dynamic cable system components.....	22
Figure 5-2: Dynamic cable system with mooring lines.....	23
Figure 5-3: Typical bend stiffener used in the design .....	24
Figure 5-4: Tensions of the cable observed against arc length.....	25
Figure 5-5: Maximum curvature envelope of cables IAC00 and IAC01 .....	26
Figure 6-1 IAC layout .....	32

## List of Tables

Table 1-1: Drag forces on the VoltturnUS-S semi-submersible platform .....	5
Table 1-2: Global quadratic damping coefficients for VoltturnUS-S semi-submersible platform.....	5
Table 1-3: Assumed thickness of marine growth at depth ranges .....	6
Table 1-4: Omnidirectional current extremes at the site (Cheynet, Li, & Z., 2024) .....	8
Table 1-5: Summary of DLCs .....	9
Table 1-6: Metocean conditions and design load case summary .....	9
Table 3-1: Mooring Azimuth for ULS for the site .....	13
Table 3-2: Mooring properties for the site.....	14
Table 3-3: Mass and drag coefficients of mooring components.....	14
Table 3-4: Mooring system ULS results: Design tensions .....	15
Table 3-5: Mooring system ULS results: Utilisation ratios.....	15
Table 3-6: Mooring system ULS results: Substructure Offsets.....	15
Table 4-1 Empirical Parameters ‘a’ and ‘b’ (American Bureau of Shipping (ABS), 2013) .....	18
Table 4-2: Summary of anchor design tensions (including safety factors) .....	18
Table 4-3: Properties of the Vryhof Stevpris MK6 drag anchor .....	19
Table 5-1: Properties of the dynamic cable system for site Utsira Nord.....	23
Table 5-2: Properties of the dynamic cable used.....	24
Table 5-3: Properties of bend stiffener used.....	24
Table 5-4: Properties of equivalent buoyancy element line type .....	25
Table 6-1 Sector-wise Weibull distribution parameters at hub height (150 m) at the Utsira Nord site .....	27
Table 6-2 Cable Sizing per String .....	33
Table 6-3, Cable lengths.....	33
Table 6-4 Cable lengths for static and dynamic cables .....	34

## List of Acronyms

AEP	Annual Energy Production
ALS	Accidental Limit State
DFE	Design Fatigue Factor
DLC	Design Load Case
ECM	Extreme Current Value
EOL	End-of-life
ESS	Extreme sea-state
EVA	Extreme Value Analysis
EYA	Energy Yield Assessment
FLS	Fatigue Limit State
FOWA	Floating Offshore Wind Arrays
GDG	Gavin & Doherty Geosolutions
HDB	Hydrodynamic Database
HOP	Hang-off Point
H <sub>s</sub>	Wave Significant Height
IAC	Inter-Array Cable
IDEA	Integrated Design of floating wind arrays - IEA Wind Task 49
ILA	Integrated Load Assessment
LCOE	Levelised Cost of Energy
LCT	Load Case Tables
LRD	Load Reduction Device
MBL	Minimum Breaking Load
MBR	Minimum Bending Radius
MDA	Maximum Dissimilarity-based Algorithm
MG	Marine Growth
MSP	Marine Spatial Planning
NCM	Normal Current Value
NSS	Normal sea-state
NORA3	3-km Norwegian Reanalysis
OWF	Offshore Wind Farm
POT	Peak-over-threshold
QTF	Quadratic Transfer Function
RFA	Reference Farm Array
SF	Safety Factor
SLSQP	Sequential Least Squares Programming
SOL	Start-of-life
SSS	Severe sea-state
T&I	Transportation and Installation
TDP	Touchdown Point
T <sub>p</sub>	Wave Period
UCC	University College Cork
UHC	Ultimate Holding Capacity
ULS	Ultimate Limit State
WTG	Wind Turbine Generator

# 1 Introduction

This report focuses on Reference Farm 9 located at Utsira Nord, Norway which has an intermediate water depth of 300 m. It has a capacity of 1 GW, with 67 semi-submersible platforms supporting 15 MW wind turbines and station-keeping composed of catenary chain-wire lines and drag embedment anchors.

## 1.1 VoltornUS-S semi-submersible platform

The VoltornUS-S steel semi-submersible substructure is taken as the baseline floating substructure to be used in this work. Details of the substructure are provided in the reference report (Allen, et al., 2020). The simulation model is a modified version of Orcina's example model (Orcina Ltd, n.d.).

### 1.1.1 Hydrodynamic properties

The original Orcina model is a pure potential flow theory hydrodynamic database (HDB) model with additional viscous damping modelled by global loads only. For this study the semi-submersible substructure is modelled as a hybrid HDB and strip theory model, with horizontal drag forces on the columns and pontoons modelled by Morrison's equation. The primary purpose of this modification is to include the effect of wind and current drag forces on the substructure, which are significant for station-keeping and dynamic cable design. Drag coefficients are extracted from DNV-RP-C205 (DNV, Recommended Practice Environmental Conditions and Environmental Loads DNV\_RP\_C205, 2021) as shown in Table 1-1.

**Table 1-1: Drag forces on the VoltornUS-S semi-submersible platform**

Element	Transverse Drag Coefficient
Central Column	1.192
Outer Column	0.972
Pontoon	1.728

Global quadratic coefficients are then tuned in order to provide free decay responses similar to the original model. The resultant coefficients are shown in Table 1-2.

**Table 1-2: Global quadratic damping coefficients for VoltornUS-S semi-submersible platform**

Element	Original	Updated	Units
Surge	922.5	115.3	kN/(m/s) <sup>2</sup>
Sway	922.5	115.3	kN/(m/s) <sup>2</sup>
Heave	2296	2296	kN/(m/s) <sup>2</sup>
Roll	16.76e6	16.76e6	kN.m/(rad/s) <sup>2</sup>
Pitch	16.76e6	16.76e6	kN.m/(rad/s) <sup>2</sup>
Yaw	47.98e6	0	kN.m/(rad/s) <sup>2</sup>

### 1.1.2 WTG Controller

The controller for the 15 MW reference WTG on the VoltturnUS-S semi-submersible substructure is unmodified from the reference model. The floating feedback loop (Fl\_Mode) uses the nacelle rotational velocity, with the proportional feedback gain term (Fl\_Kp) set at -9.26.

## 2 Site Conditions

The Utsira Nord site is located within the Norwegian Economic Zone, 22 km off the Norwegian coast, with an area of 1010 km<sup>2</sup> and bathymetric water depths ranging from 185-280 m. For the purpose of generalisation, a constant water depth of 300 m is assumed for this project. In 2022, the Norwegian government proposed a total installed capacity of 1.5 GW for Utsira Nord (Cheynet, Li, & Z., 2024).

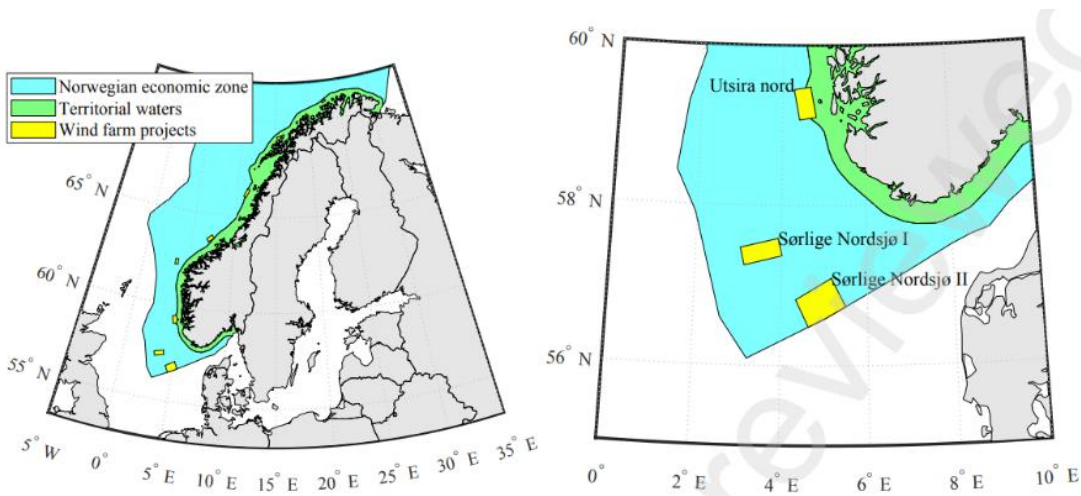


**Figure 2-1: The Norwegian economic zone with proposed offshore wind farm projects (left) and the Utsira Nord site (right)**

The site is just above 59° N, where the recommended marine growth switches from 100 mm to 50 mm (DNV, Position Mooring DNV-OS-E301, July 2021). For the sake of conservatism at this early design stage, 100 mm marine growth is assumed. Zero marine growth was assumed below a depth of 170 m, based on the data in (Devantier, Wong, & Schrameyer, 2024). This adjustment eases the design of the dynamic cable S bend, allowing the buoyancy modules to be below the marine growth water depth. The marine growth thickness and depth ranges are shown in Table 2-1. The density of marine growth is 1300 kg/m<sup>3</sup> (DNV, Position Mooring DNV-OS-E301, July 2021).

**Table 2-1: Assumed thickness of marine growth at depth ranges**

Depth range	Marine growth thickness (mm)
Surface to 40 m	100
40 m to 170 m	50
Below 170 m	0

### 2.1 Metocean Conditions

The wind and wave conditions were obtained from the publicly available NORA3 (3-km Norwegian Reanalysis) database (Institute, n.d.). Both the wind and wave data have a spatial resolution of 3 km

and a temporal resolution of 1 hour. Metocean analysis of the 1-hour data was carried out as in (Creane, 2024)

Since the reference site covers a large area, the spatially averaged wind and wave data of the whole area were analysed. The resultant wind and wave rose diagrams are presented in Figure 2-2. The current profile used in the project can be seen in Table 2-2.

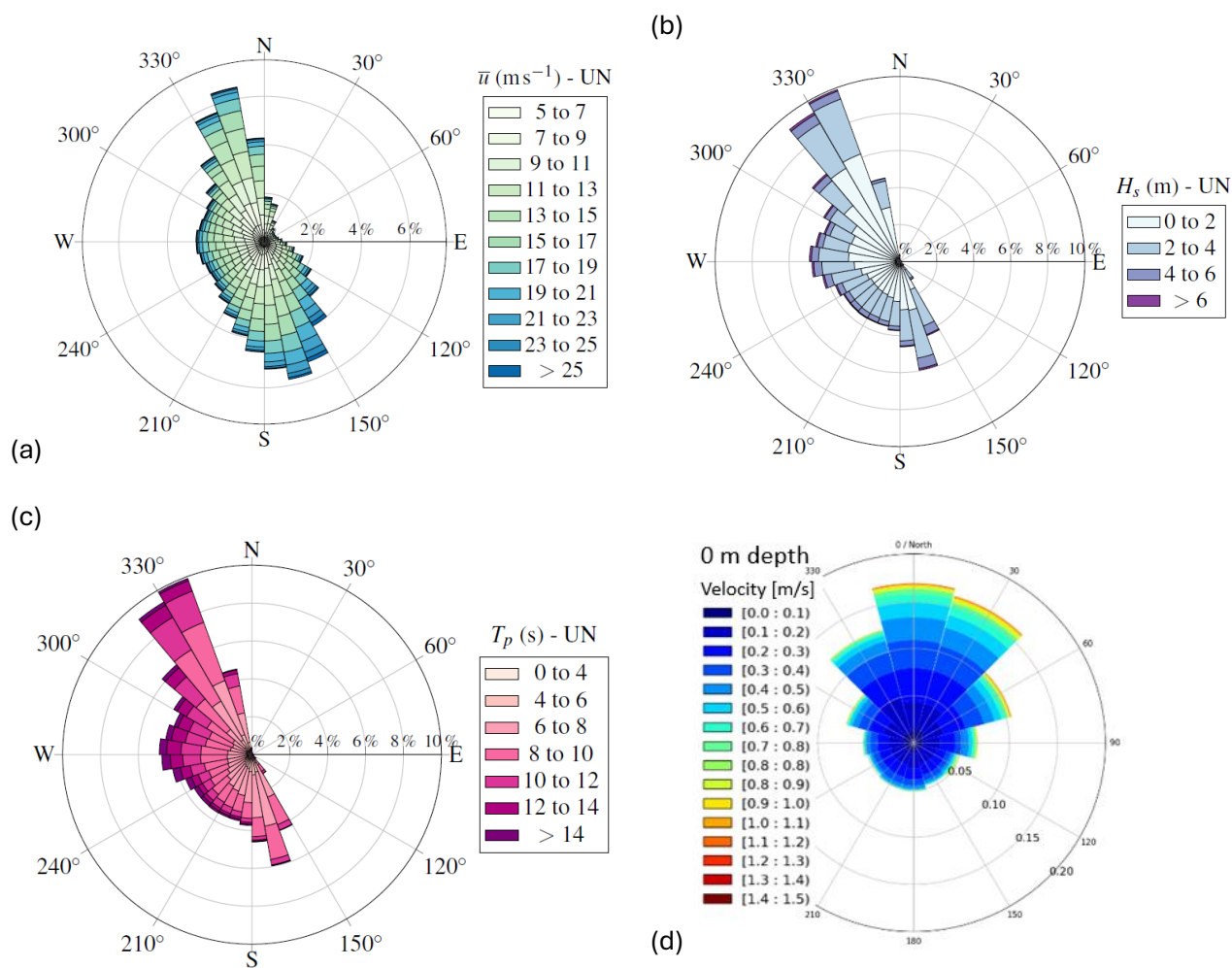
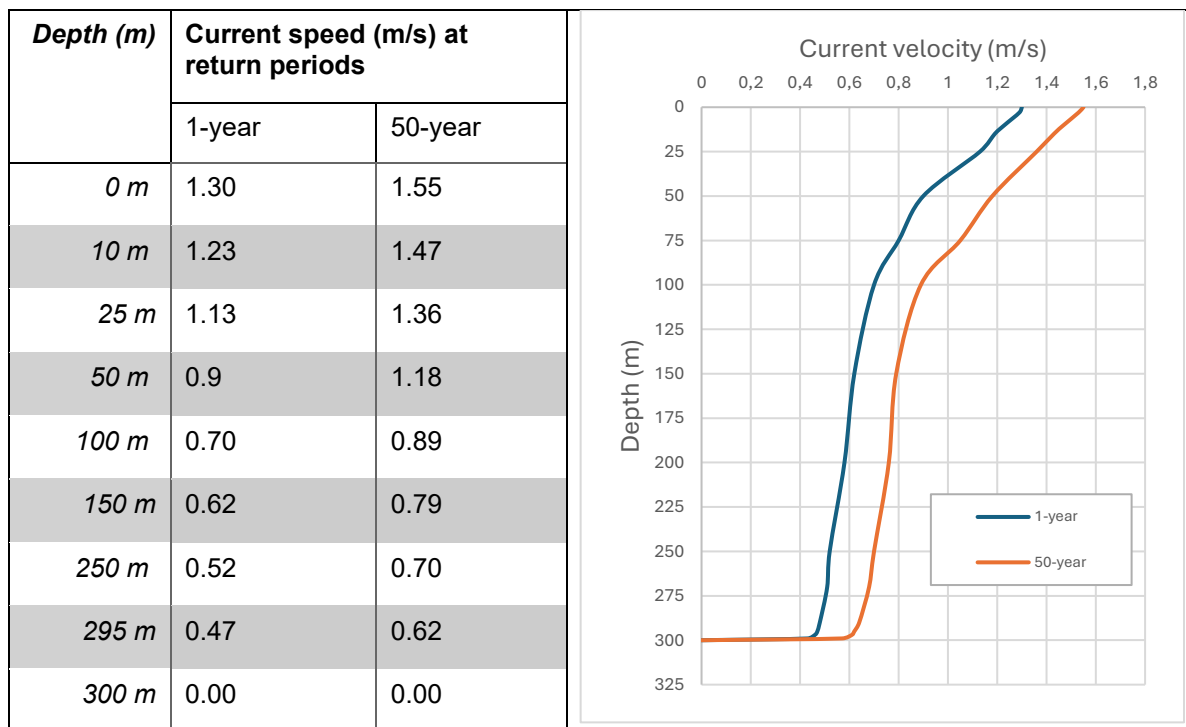


**Figure 2-2: Metocean data: (a) Mean wind speed at height 150 m, (b) Significant wave height  $H_s$ , (c) Spectral Peak Period  $T_p$  and (d) Current velocity at 0 m depth**

**Table 2-2: Omnidirectional current extremes at the site (Cheynet, Li, & Z., 2024)**



## 2.2 Ground Conditions

This section presents a summary of the ground conditions at the Utsira Nord site. Further details can be found in (Rezaeifar, 2025).

The modified seafloor sediment maps indicated that most of the seabed within the site’s boundaries is composed of Weichselian and early Holocene silt/clay. Site investigations confirmed that the site’s top layers range between marine very soft to firm sandy silty clay. The layers below these have been interpreted as muddy sand underlain by coal pit formation, which is interpreted as glaciomarine sandy silty clay.

The ground conditions at this site indicate that the founding stratum can be simplified to soft clay.

## 2.3 Design Load Case

In this section, the design load cases (DLC) used in the project for Utsira Nord site are described (Hall, et al., June 2024).

As this is a research-oriented study, a greatly reduced set of DLCs was selected to manage computational costs and simulation time. Specifically, the analysis focused on ultimate limit state (ULS) conditions using DLCs 1.6 and 6.1, and fatigue limit state (FLS) conditions using DLC 1.2. A summary of the DLCs with each limit state condition can be seen in Table 2-3.

**Table 2-3: Summary of DLCs**

Design condition	DLC	Wind condition	Waves	Currents	Type of analysis
Power production	1.2	NTM $V_{in} < V_{hub} < V_{out}$	NSS Joint probability distribution	NCM	Fatigue
Power production	1.6	NTM $V_{Rated}$	SSS $H_s = H_{s, SSS}$	NCM	Ultimate
Idling	6.1	EWM $V_{hub} = V_{ref}$	ESS $H_s = H_{s50}$ , $H_{max} = 1.86H_s$	ECM $U = U_{50}$	Ultimate

For the ULS analysis, DLC 1.6 represents the wind turbine operating under rated wind speed conditions in a severe sea state (SSS), while DLC 6.1 captures the turbine in an idling state during an extreme sea state (ESS). The wind conditions for DLC 6.1 are based on site-specific, unidirectional 50-year return period wind speeds. As the maximum wave height during the ESS was shown to govern the mooring design, the anomaly index of 1.86 as specified by (IEC, 2019) was taken.

For the FLS analysis, DLC 1.2 was considered. DLC 1.2 corresponds to the turbine operating under normal conditions in normal sea states (NSS). It must be ensured that the number and resolution of the NSS considered are sufficient to account for the fatigue damage associated with the full long-term distribution of metocean parameters. The  $H_s$ ,  $T_p$ , wave and wind direction for each NSS shall be considered, together with the associated mean wind speed, based on the long-term joint probability distribution of metocean parameters.

**Table 2-4: Metocean conditions and design load case summary**

	DLC 1.6	DLC 6.1
Wind speed (m/s)	10.59	37.5
Turbulence intensity	0.06	0.05
Shear	0.14	0.11
Wave height (m)	8.32	14.4
Wave period (s)	12.75	16.5
Current speed (m/s)	1.30	1.55

It is important to note that, in a commercial design process, a comprehensive set of DLCs would typically be evaluated to ensure the robustness and reliability of the design across all relevant scenarios. As such, the reduced set here represents a limitation of the study, and certain critical loading conditions or failure modes may not be captured in the current analysis.

The design of mooring lines considers ULS and FLS cases, whereas the anchor and dynamic cable designs consider only ULS cases.

For the fatigue load cases, 100% WTG and substructure availability is assumed. Consequently, whenever wind speeds fall within the operational range, the WTG is simulated in power production mode. No downtime is considered. This can be considered as generally conservative as the operational wind turbine has larger wind loading compared to an idling or parked wind turbine.

No WTG yaw misalignment is considered in this work.

### 2.3.1 Fatigue binning

A joint probability analysis of the combined wind and wave conditions for the Utsira site was conducted using the Maximum Dissimilarity Approach (MDA) and hindcast data. The MDA approach, unlike conventional rectangular clustering or binning of metocean environmental conditions determines clusters based on the proximity between data points and does not need to follow the hyper-cube approach, allowing for more efficient coverage of the data distribution.

The use of clustering for metocean conditions of floating wind turbines has been demonstrated in the past (Kanner, Aubault, Peiffer, & Yu, 2018) and showed that clustering can provide comparable fatigue results while reducing the amount of analysis points by multiple orders of magnitudes compared to rectangular binning.

Fatigue binning for the wind and wave data has been considered on five environmental parameters: significant wave height, wave peak period, wind speed, wind direction, and wave direction. The scatter plots for these parameters against wave significant wave height have been presented in Figure 2-3. These fatigue binning analyses do not consider current data, as it is assumed negligible for fatigue calculations.

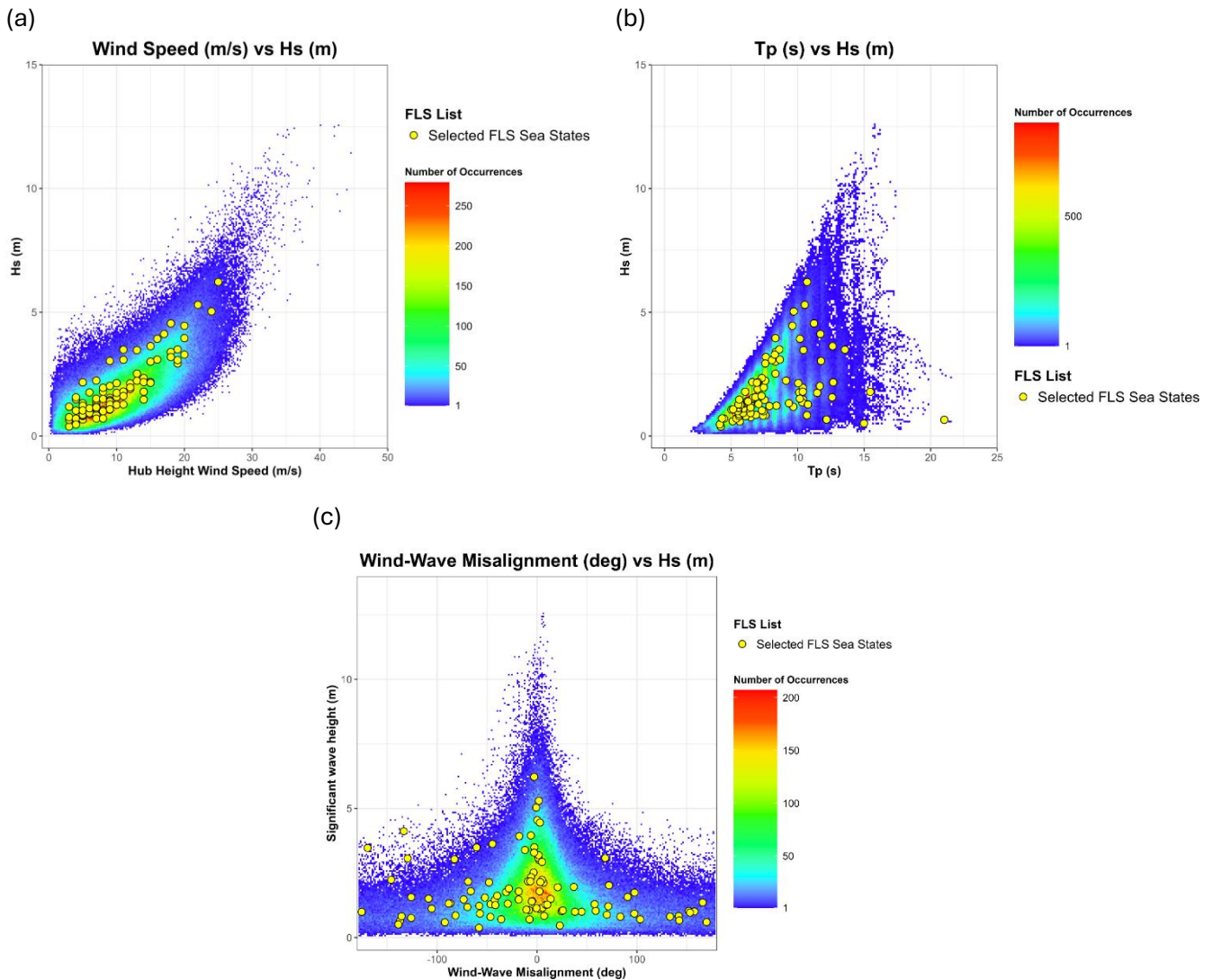
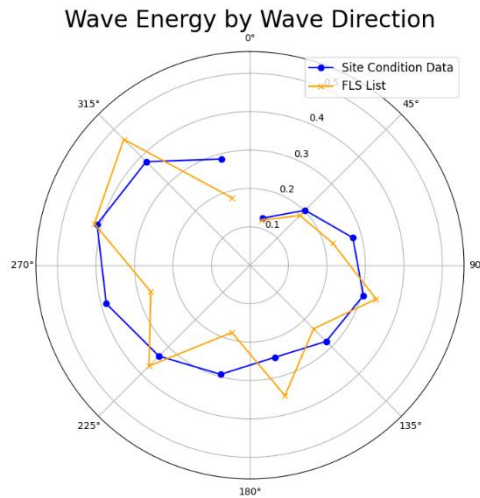


Figure 2-3: Kernel density plots of Wave Significant height ( $H_s$ ) and (a) Wind speed, (b) Wind-wave misalignment and (c) Peak Period ( $T_p$ )

It can be seen in Figure 2-3 (a), (b) and (c) that the selected FLS sea states represent the site conditions well for wind speeds between 2 and 20 m/s, and peak periods ( $T_p$ ) between 4-15 s and the wind-wave misalignment angles, respectively.



**Figure 2-4: Rose plot of the Wave Energy by Wave direction**

The results from the binning of FLS data have also been summarised in the form of scatter plots of the environmental parameters relative to one another. These can be found in Appendix A, along with the overall distribution of environmental parameters as a function of percentage of occurrence.

### 3 Mooring Design

An overview of the mooring design methodology and resultant designs are presented in this section. Further details on the methodology can be found in (Hall, et al., June 2024).

The general mooring design philosophy is as follows:

- To be compliant with ULS and FLS design requirements
- To limit the maximum substructure offset to no more than 35% of the water depth at each site (as dynamic cable configurations are not available at the mooring design stage)
- To minimize the number of mooring lines
- To minimize the required chain diameter
- To use the same mooring configuration for all units in the array, only varying the mooring heading

Other valid design approaches that were not used include limiting mooring component sizes to those with a greater production capacity or transportation and installation (T&I) marine spread availability.

The working group selected a chain – wire rope catenary as the base case for this reference design.

For the mooring design, DLC 1.6 and 6.1 are considered for ULS and DLC 1.2 is considered for FLS.

### 3.1 Simulation

Mooring simulations are run using Integrated Load Assessment (ILA) for ULS in OrcaFlex (v11.4 and v11.5) and for FLS using OpenFAST. The duration is set as 4200 s to account for 300 s ramp up time, 300 s transient time, and 3600 s (1 hour) of analysis time. All simulations are run considering full marine growth.

The FLS simulations were carried out using the aero-hydro-servo-elastic tool OpenFAST, with the mooring system modelled using MoorDyn. The turbulence intensity of the wind fields was increased to account for the increased fatigue loading due to the surrounding WTG's wakes as described in (Hall, et al., June 2024).

In the case of ULS simulations, six random wave and wind seeds are run. To limit the number of simulations for FLS, a single seed is run. For FLS conditions, the wave seed is varied per sea-state, while the wind seed is kept constant per wind speed. Using a single seed per wind speed reduces the number of full wind field files required for the simulations and thus the time required to generate them. In order to use a single wind field file per wind speed, the wind speeds are rounded to the nearest whole number.

Full turbulent wind fields are generated for both ULS and FLS conditions using TurbSim (v2.0) (B. J. Jonkman, 2016).

Mooring properties including drag coefficients are selected dependent on the mooring line type from (DNV, Position Mooring DNV-OS-E301, July 2021) and added mass coefficients from (Vertias, July 2021). For the sake of simplicity, the additional clump weight modules are only modelled as mass elements, neglecting hydrodynamic forces.

### 3.2 Design Criteria

ULS design tensions are calculated as per DNV (DNV, Position Mooring DNV-OS-E301, July 2021) on both the chain and wire rope components. ULS checks on the chain assume 100% corrosion allowance. Considering the research nature of the project, the design tension is taken conservatively as the maximum of the six random realisations.

FLS checks are calculated considering the chain at 50% corrosion allowance and calculated according to API ((API), 2005). The design fatigue factor (DFF) is taken as 5 (non-inspectable).

### 3.3 Description of Mooring System

A three-line catenary chain, wire and clump weight mooring design is proposed for the site. Mooring properties are shown in Table 3-1 and Table 3-2. Fairlead to anchor radius is set at 979.6 m. The design is conservatively checked assuming full marine growth. The clump weight is positioned at the chain-wire interface and is sized at 80 tons to ensure positive tension always remains in both the wire and chain. Pretension (including marine growth) is 284.5 and 152.4 tons with and without clump weights respectively.

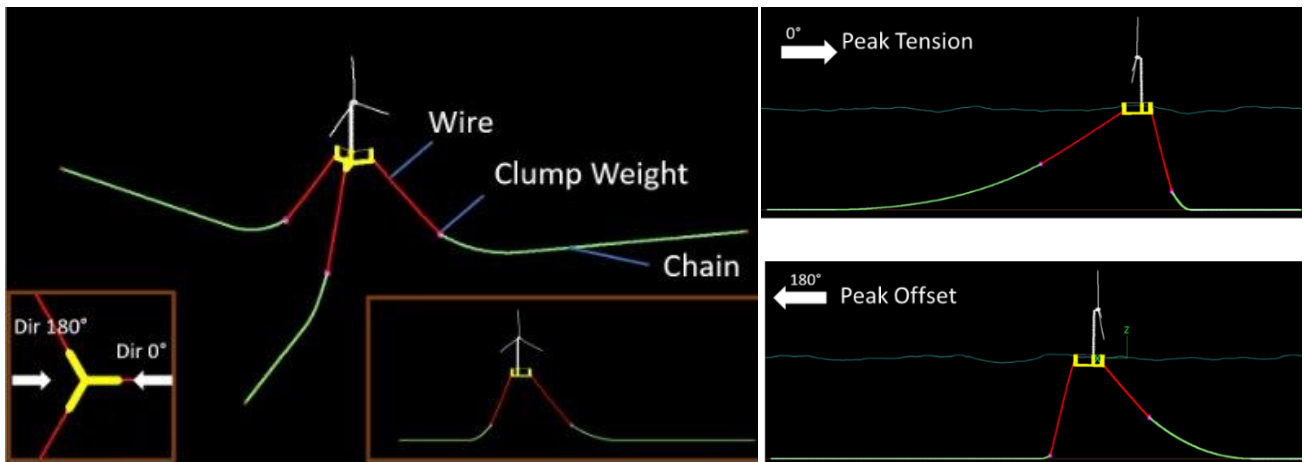


Figure 3-1: Description of mooring system

Table 3-1: Mooring Azimuth for ULS for the site

Utsira (Intermediate) Mooring Azimuth for ULS

	Line 1	Line 2	Line 3	Units
<b>Mooring Azimuth</b>	0	120	240	°

**Table 3-2: Mooring properties for the site**

**Utsira (Intermediate) Mooring properties**

Section	Parameter	Line 1, 2 & 3	Units
<b>Overall</b>	Mooring Radius	979.6	m
	Pretension (with clump weight)	2789.9	kN
	Pretension (without clump weight)	1494.6	kN
<b>Wire</b>	Length (Unstretched)	280.0	m
	Nominal Diameter	160.0	mm
	Dry mass (without marine growth)	135.5	kg/m
	Type and grade	Sheathed spiral strand wire	/
	MBL	26163.2	kN
<b>Clump Weight</b>	Mass	80000.0	kg
	Position	At chain-wire interface	/
<b>Chain</b>	Type and grade	Studless R4	/
	Length (Unstretched)	817.0	m
	Nominal Diameter	175.0	mm
	Dry mass (without marine growth)	612.5	kg/m
	MBL (fully corroded)	22508.4	kN

**Table 3-3: Mass and drag coefficients of mooring components**

Mooring component	Water depth	Parameter	Value
<i>Chain (no marine growth - refer to Table 2-1)</i>	>170m	Drag Coefficient (Normal)	2.40
		Drag Coefficient (Axial)	1.15
		Added mass coefficient (Normal)	1.00
		Added mass coefficient (Axial)	0.50
<i>Wire (with marine growth)</i>	<40m	Drag Coefficient (Normal)	2.10
		Drag Coefficient (Axial)	0.00
		Added mass coefficient (Normal)	1.00
		Added mass coefficient (Axial)	1.00
	40-170m	Drag Coefficient (Normal)	1.65
		Drag Coefficient (Axial)	0.00
		Added mass coefficient (Normal)	0.00
		Added mass coefficient (Axial)	0.00
	>170m	Drag Coefficient (Normal)	1.20
		Drag Coefficient (Axial)	0.00
		Added mass coefficient (Normal)	0.00
		Added mass coefficient (Axial)	0.00

### 3.4 Mooring ULS Results

The results of the mooring ILA are presented in this section.

**Table 3-4: Mooring system ULS results: Design tensions**

DLC	Component	Line 1	Line 2	Line 3	Units
1.6	Sheathed spiral strand wire	12454	9338	9376	kN
	Studless Chain	11651	8542	7463	kN
6.1	Sheathed spiral strand wire	18140	13750	13874	kN
	Studless Chain	17496	13018	12056	kN

The peak design tension observed for the mooring systems is 18.14 MN (observed on Line 1), while the minimum line tension is 7.46 MN (observed on Line 3). The bottom of the wire rope section maintains a seabed clearance of 7 m in all conditions.

**Table 3-5: Mooring system ULS results: Utilisation ratios**

DLC	Component	Line 1	Line 2	Line 3	Units
1.6	Sheathed spiral strand wire	0.48	0.36	0.36	Utilisation Ratio
	Studless Chain	0.52	0.38	0.33	Utilisation Ratio
6.1	Sheathed spiral strand wire	0.69	0.53	0.53	Utilisation Ratio
	Studless Chain	0.78	0.58	0.54	Utilisation Ratio

**Table 3-6: Mooring system ULS results: Substructure Offsets**

DLC	Offset (m)	Offset (% Water Depth)
1.6	83.5	28
6.1	97.2	32

The maximum ULS conditions occur in DLC 6.1, producing a peak offset of 97.2 m (32% water depth) and peak utilisation factors of 0.69 and 0.78 for the sheathed wire and chain respectively.

### 3.5 Mooring FLS Results

A fatigue damage analysis was carried out to determine if the mooring system would withstand the expected lifetime fatigue load. The fatigue load cases were defined using the output from the fatigue binning analysis. The fatigue lifetime of the mooring system is 25 years. The T-N curve of a studless chain, as defined by the API standard ((API), 2005), is used for the fatigue analysis as shown in the following equation with slope  $m$  equals 3 and intercept  $k_{T-N}$  equals 316. The MBL used accounts for 50% of the corrosion allowance of the steel chains. The tension is taken at the wire-chain interface location.

$$N = k_{T-N} \left( \frac{Tension}{MBL} \right)^{-m}$$

Afterwards the damage of each fatigue bin  $D_i$  was obtained and used in calculating the lifetime fatigue damage  $D_{25-years}$  as shown in the following equation:

$$D_{25-years} = \frac{T_{25-years}}{T_{sim}} \sum_{i=1}^{bins} f(bin)_i D_i$$

Where  $T_{sim}$  is the simulation time of 3600 s, and  $f(bin)_i$  is the probability of occurrence of each fatigue bin  $i$ . A design safety factor of 5 was used, hence for a mooring system to pass the fatigue design limit, the lifetime fatigue damage has to be lower than 0.2.

The goal of the FLS analysis was to assess the fatigue damage of the mooring system at all possible headings, this can be used further during the wind farm layout design to identify the possible orientation of the mooring system. Since the mooring system is symmetric, 12 simulations were carried out with a step of 10°. Where 0° and 10° heading is shown in the following Figure. Similarly, 20° heading would be rotating the mooring system anticlockwise with another 10°. The mooring system headings affect the way the load is shared across the 3-mooring system, an identical case would be to find an orientation where the lifetime fatigue damage is equally distributed over the three mooring lines. The distribution of the fatigue damage over the lines depends on the fatigue bins coming from the metocean conditions from the site and the orientation of the mooring system inside the wind farm. Hence the orientation of the mooring system inside the farm can be optimized to decrease the fatigue damage on the mooring system.

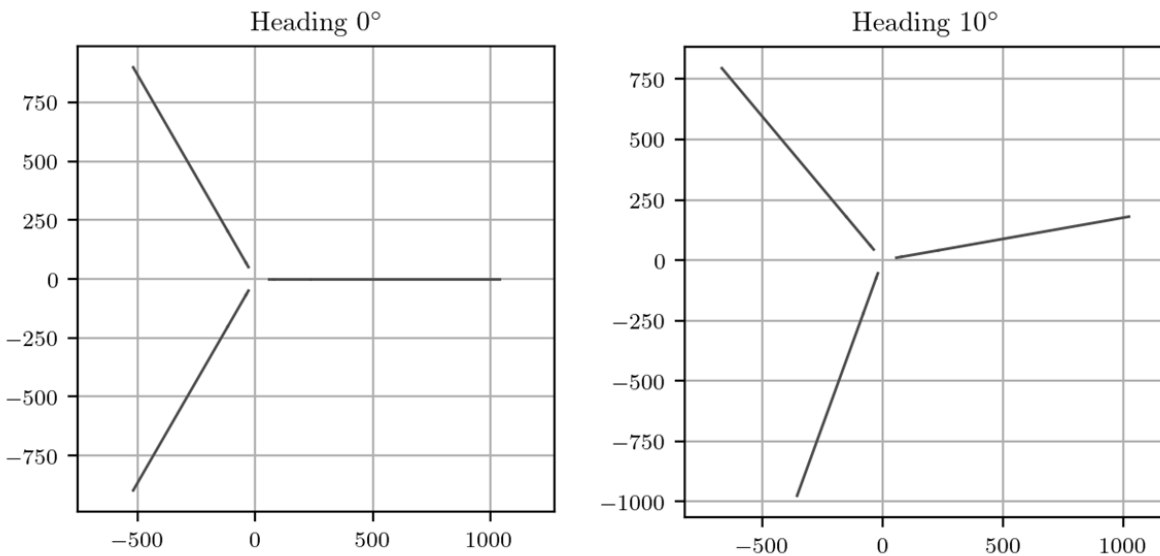


**Figure 3-2: Mooring system headings at 0° (left) and 10° (right)**

The results of the FLS analysis is shown in Figure 3-3, where all orientations, with the exception of heading 0°, and heading 60°. successfully passing the design limit. The lowest value of lifetime fatigue damage was around a mooring system heading between 20° and 30°.

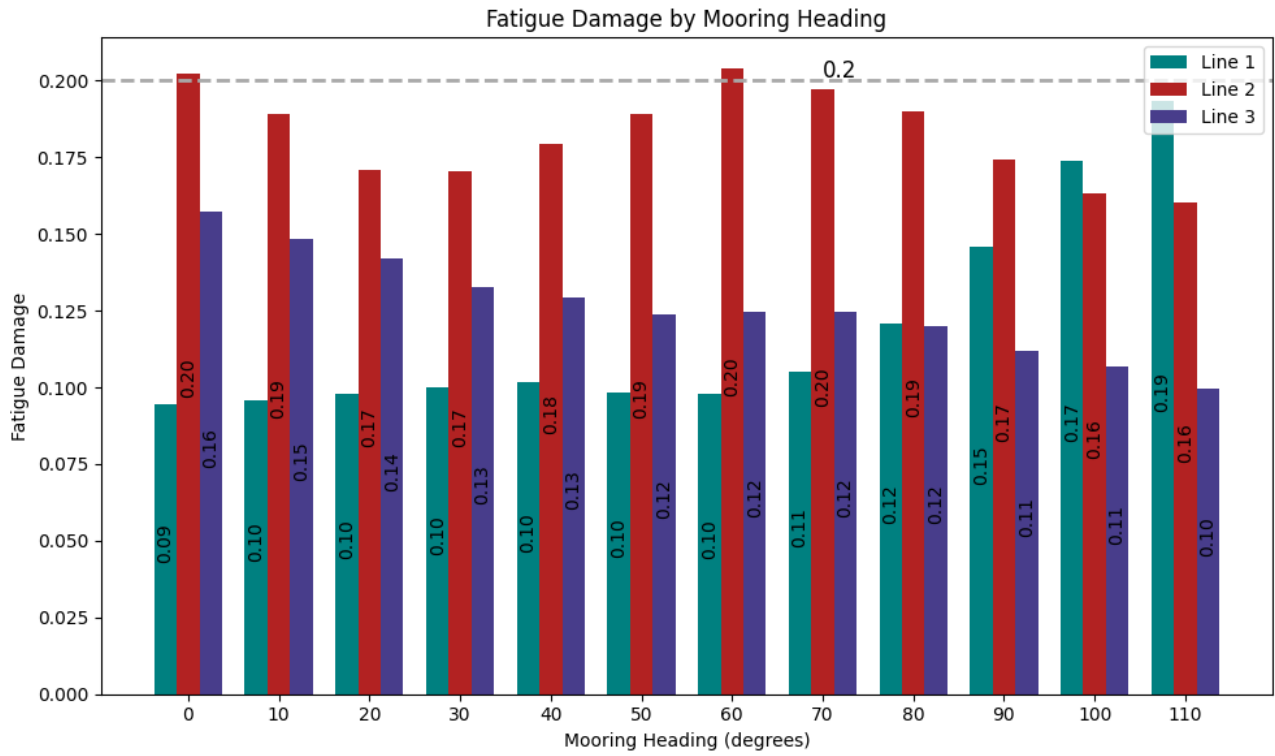


Figure 3-3: Lifetime fatigue damage at all possible mooring headings

## 4 Anchor Design

### 4.1 Methodology

The drag anchor size was determined using the empirical correlation for Vryhof Stevpris drag anchors (American Bureau of Shipping (ABS), 2013):

$$UHC = a(W)^b$$

where,

UHC:	Ultimate holding capacity (kN)
a, b:	Empirical parameters based on the soil type (-)
W:	Weight of the anchor (t)

At this site, the maximum factored anchor tension load from the mooring analysis was taken as the UHC. For this analysis, the Vryhof Stevpris MK6 anchor was considered.

The values for the empirical parameters  $a$  and  $b$  are detailed in Table 4-1. These parameters were chosen based on the soil type at the site

**Table 4-1 Empirical Parameters ‘a’ and ‘b’ (American Bureau of Shipping (ABS), 2013)**

Soil Type	a	b
Very Soft Clay	509.96	0.93

### 4.2 Loading

The anchor design tensions including safety factors are summarised below in Table 4-2:

**Table 4-2: Summary of anchor design tensions (including safety factors)**

DLC	Line 1	Line 2	Line 3	Units
1.6	6722	4939	4969	kN
6.1	15887	12037	12765	kN

The maximum factored anchor tension load from the mooring analysis indicated a load of 15,887kN at the anchor point.

### 4.3 Sizing

The ground conditions at this site indicate that the founding stratum can be simplified to soft clay suitable for a drag anchor. Using the equation presented in Section 4.1, the resulting weight of the drag anchor is 40.36t. The dimensions of the anchor corresponding to this weight were derived from the Vryhof Manual. The overall length of the anchor is 9.70 m, with the Fluke length and Fluke width equal to 6.87 m and 10.84 m respectively. Further properties of the anchor have been summarised in Table 4-3.

**Table 4-3: Properties of the Vryhof Stevpris MK6 drag anchor**

**Vryhof Stevpris MK6 Drag Anchor**

<b>Weight (kg)</b>	<b>Penetration (m)</b>	<b>Drag in mrt (m)</b>	<b>UHC (mT)</b>
<b>40,360.0</b>	23.5	120.0	1600.0

For very soft clays (mud), the recommended optimal fluke/shank angle is 50° (American Bureau of Shipping (ABS), 2013).

## 5 Dynamic Cable Design

### 5.1 Overview

This section outlines the methodology adopted for the design of the dynamic power cable system within the context of this research project. The approach is intentionally simplified and modular to support early-phase design studies and to enable rapid iterations during conceptual development. The methodology integrates key engineering objectives with practical constraints representative of floating offshore wind environments.

The cable design philosophy implemented in this study is guided by the following core principles:

- Establishment of an Optimized Lazy Wave Configuration
- Minimization of Cable and Ancillary System Lengths
- Clearance from Sub-sea Structures and System Integration
- Structural Integrity under Extreme Environmental Conditions
- Seabed and Water Column Clearance

This methodology enables a practical yet technically sound pathway for designing dynamic cable systems in early-stage projects, while aligning with industry best practices and facilitating future refinement for detailed engineering.

### 5.2 Design Procedure

The design of dynamic power cables for floating offshore wind turbines follows a staged process integrating analytical modelling, iterative verification. This methodology ensures that mechanical performance (tension and curvature) and fatigue life comply with design limit states. The design process comprises four main stages: Initial Design, Basic Design, Design Verification, and Final Design. Each stage is supported by specific input data and modelling efforts, as outlined below.

- The following parameters must be collected prior to initiating the design process:
- Environmental conditions (wave, wind, current)
- Power cable specifications (cross-section, materials, mechanical properties)
- Floating platform characteristics and 6-DoF motions
- Mooring system type and stiffness
- Seabed properties (soil shear strength, slope, bathymetry)

A model of the platform and mooring system is developed to support time-domain analyses.

### 5.3 Initial Design

In the initial stage, Design Driving Load Cases (DDLCS) are defined based on preliminary metocean conditions and operational profiles.

Key activities:

- **Static Analysis:** Sensitivity studies on hang-off point height, cable orientation, and seabed touchdown location are performed to identify feasible cable geometries.
- A preliminary set of acceptable cable combinations is developed based on allowable tension and curvature. The cable configurations are defined by using an optimisation algorithm to gain a configuration with minimum tension and curvature along the cable
- If no suitable cable design is found, adjustments are made by redefining the feasible combinations.

## 5.4 Basic Design

This stage performs a more detailed simulation under time-domain (TD) conditions for the previously selected configurations.

Key activities include:

- **Dynamic Analysis in Time Domain:** Cable configurations are evaluated under DDLs, including Ultimate (ULS).
- A set of "good" cable designs is retained if they comply with maximum tension and curvature thresholds.

If the results are not acceptable, the procedure loops back to redefine cable combinations, or in some cases, the power cable may need to be changed.

## 5.5 Design Conditions

The scope of this study is limited to evaluating the dynamic cable system under the Ultimate Limit State (ULS) condition, to assess cable integrity under extreme environmental loading. The analysis is based on Design Load Case (DLC) 6.1, which is conventionally applied to simulate severe sea states with combined wave and wind loading and aligns with the conditions defined for the mooring system.

An uncoupled analysis approach has been adopted. In this method, pre-computed time series of floater motions and mooring line tensions, obtained from external mooring simulations, are applied as boundary conditions for the dynamic cable model. This enables the dynamic response of the cable to be assessed in a representative environmental scenario without full coupling to the floating platform or mooring system.

Other DLCs and design conditions, such as the Fatigue Limit State (FLS), Serviceability Limit State (SLS), and Accidental Limit State (ALS), are not considered in this design process. This limitation reflects the early-stage and research-focused nature of the project and prioritises a conservative assessment of performance under extreme loading.

In addition, marine growth profiles are considered for the end-of-life condition.

## 5.6 Design Criteria

The following design criteria are applied to ensure the structural integrity and operational reliability of the dynamic cable system:

- **Axial Tension:** Maximum cable tension must remain below the product of the Minimum Breaking Load (MBL) and a defined safety factor (SF)
- **Bending Curvature:** Peak curvature shall not exceed the allowable limit recommended by the manufacturer to avoid structural damage and fatigue.
- **Hog Bend Clearance:** The top of the lazy wave (hog bend) must maintain a clearance of at least 10% of the water depth below the sea surface.
- **Sag Bend Clearance:** The bottom of the lazy wave (sag bend) must remain at least 10% of the water depth above the seabed to prevent contact or abrasion.
- **Interference Avoidance:** The cable must not clash with other subsea structures such as mooring lines or anchors under any operational condition.

These criteria form the basis for evaluating the cable configuration under ultimate loading scenarios.

## 5.7 Description of the Dynamic Cable System

The dynamic power cable system consists of the main cable body, a bend stiffener at the hang-off point, a distributed buoyancy module forming the lazy wave configuration. The dynamic cable system used in this project has been illustrated in Figure 5-2 and the properties of the system have been tabulated in Table 5-1.

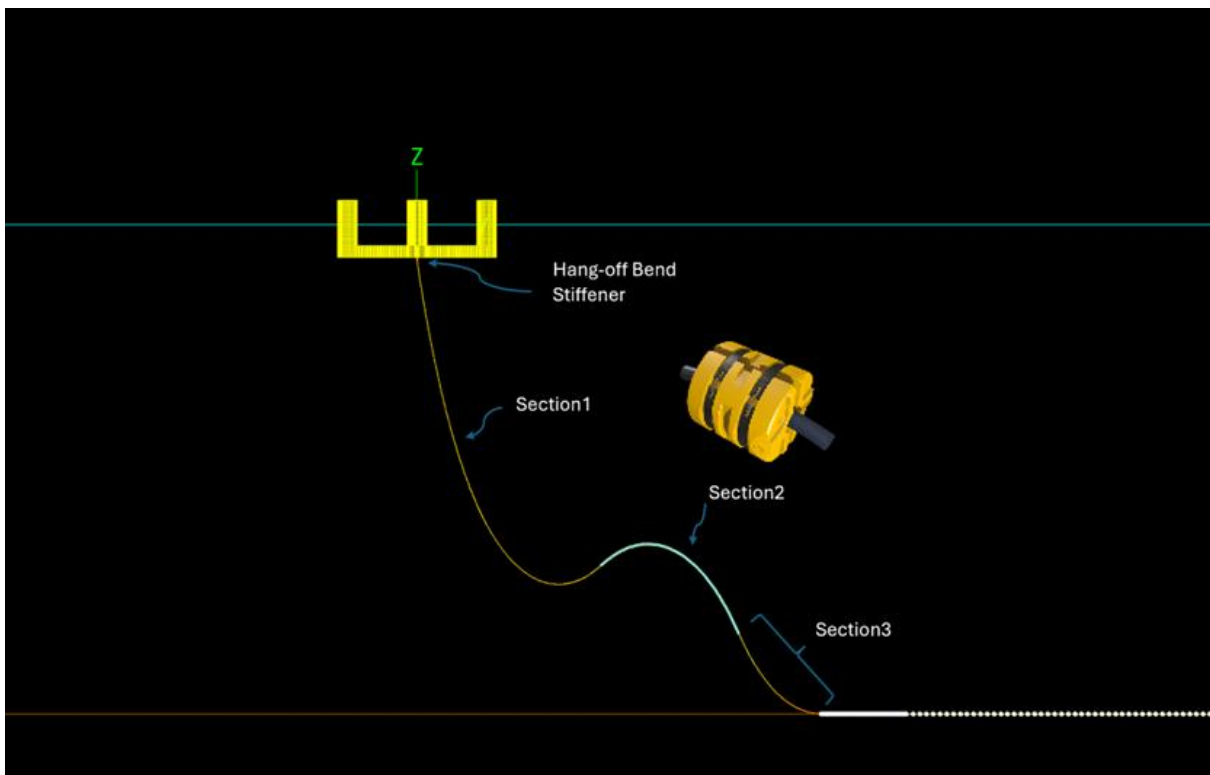


Figure 5-1: Dynamic cable system components

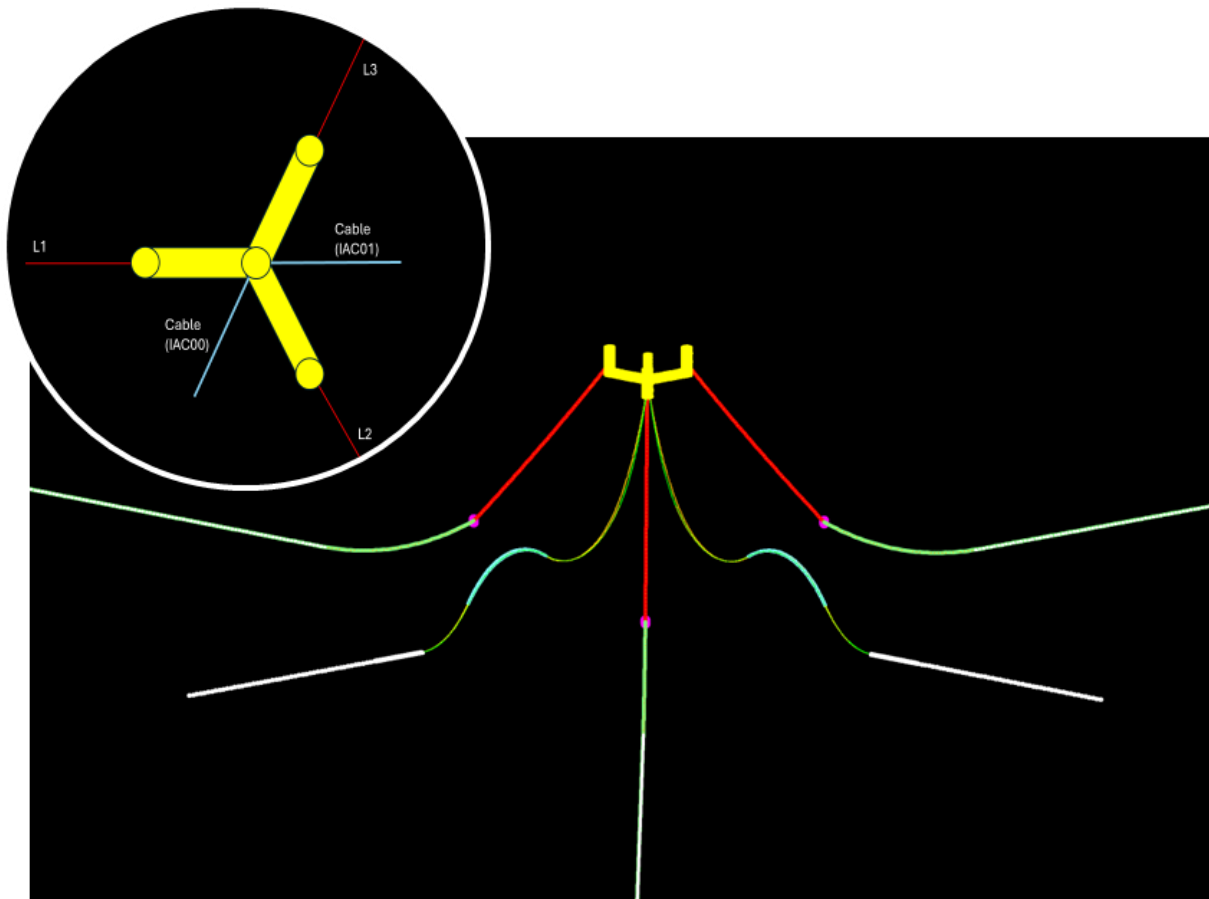


Figure 5-2: Dynamic cable system with mooring lines

Key parameters used in the model are detailed below:

Table 5-1: Properties of the dynamic cable system for site Utsira Nord

Cable Properties	Value	Unit
Section-1: Cable	275	m
Section-2: Distributed Buoyancy module	129	m
Section-3: Cable	82	m
Total length	486	m

### 5.7.1 Cable

The cable is modelled as a flexible, multilayer, non-bonded structure with properties representative of a typical medium- or high-voltage dynamic inter-array cable. The cable includes armouring layers for tensile strength and a robust outer sheath for seawater resistance.

**Table 5-2: Properties of the dynamic cable used**

Cable Properties	Value	Unit
Voltage rating	66	kV
Power	125	MW
Resistance	0.04	Ohm/km
Area	630	m <sup>2</sup>
Outer Diameter	184	m
Mass in air	55.76	kg/m
Bending stiffness	42.47	kN.m <sup>2</sup>
Axial stiffness	658	MN
Minimum Bending Radius (MBR)	2.8	m
Minimum Breaking Load (MBL)	659	kN

### 5.7.2 Bend Stiffener

A bend stiffener is applied at the hang-off location to limit curvature and provide mechanical support at the cable termination.

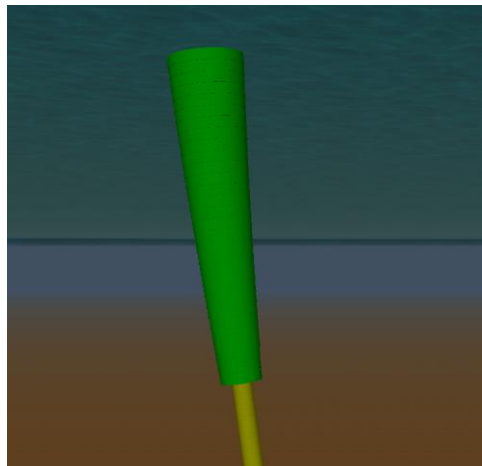


**Figure 5-3: Typical bend stiffener used in the design**

**Table 5-3: Properties of bend stiffener used**

Properties	Value	Unit
Length	4	m
Material	Polyurethane	-
OD (at 0m)	0.7	m
OD (at 4m)	0.38	m
Density	1200	kg/m
Young's modulus	45	MPa

### 5.7.3 Buoyancy Modules

Distributed buoyancy elements are applied along the midsection of the cable to form the lazy wave profile and reduce effective tension and curvature at critical locations. The equivalent line types used are shown in Table 5-4. These input parameters are used in both static and dynamic simulations to define the mechanical behaviour and geometric configuration of the cable system.

**Table 5-4: Properties of equivalent buoyancy element line type**

Properties	Value	Unit
Type	equivalent line	-
Outer diameter	0.39	m
Weight in air	948	N/m

## 5.8 Dynamic cable analysis results

Each cable was evaluated at start-of-life (SOL, without marine growth) and at end-of-life (EOL, with marine growth) conditions.

Effective tension and curvatures of cables IAC00 and IAC01 for two current directions 0° and 180°, with and without marine growth indicated by MG) are shown in Figure 5-4 and Figure 5-5.

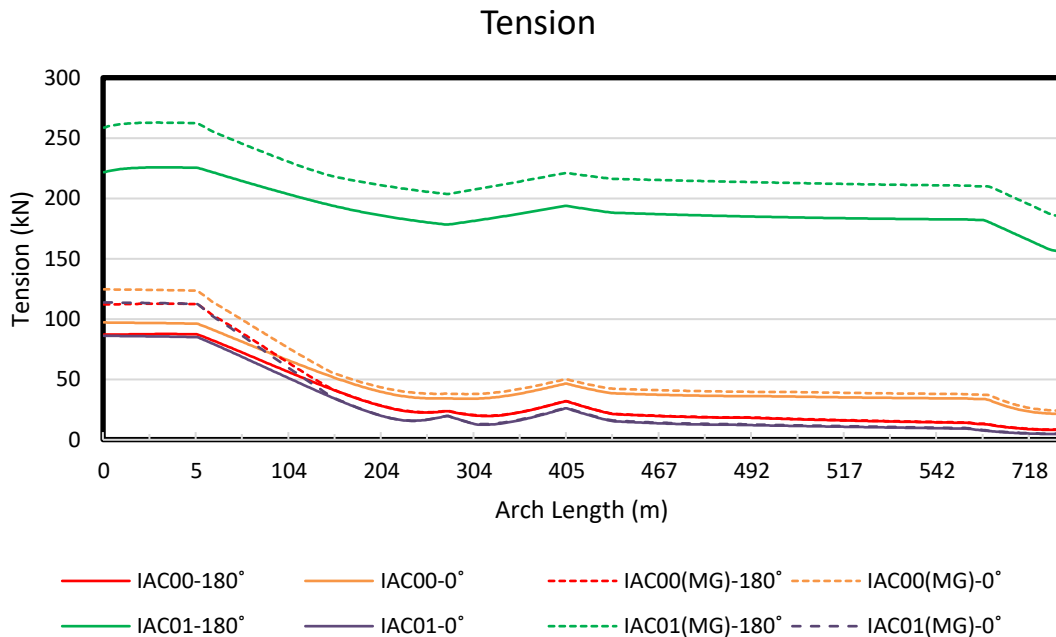


**Figure 5-4: Tensions of the cable observed against arc length**

As seen in Figure 5-4, the maximum tension is captured at a platform displacement of 92.4 m from the initial position for cable IAC01- 180. The effect of marine growth was observed as an increase in tension by 30 kN.

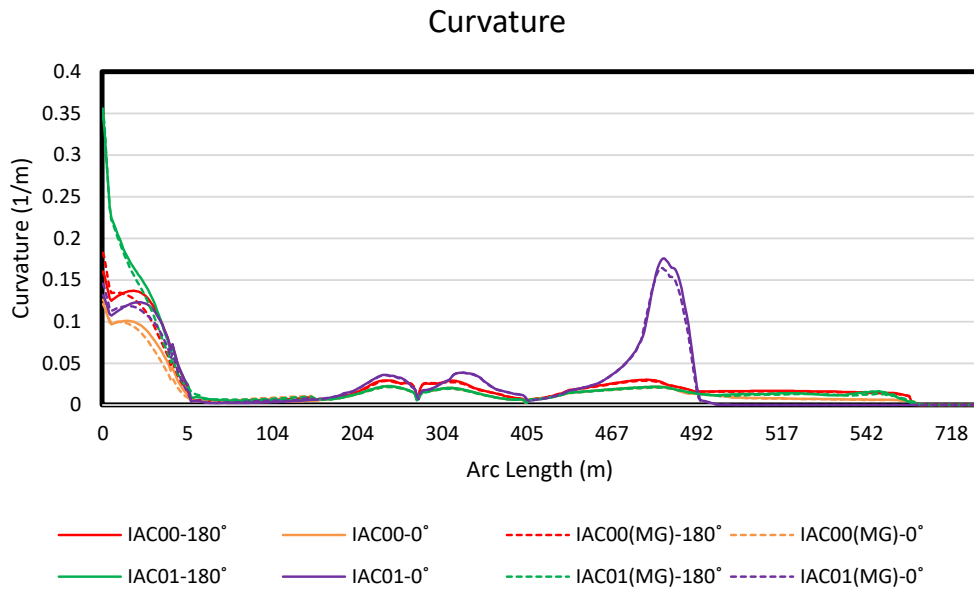


**Figure 5-5: Maximum curvature envelope of cables IAC00 and IAC01**

It can be seen from Figure 5-5 that the maximum curvature occurs at the hang-off point for cable IAC01 during 30% WD platform excursion. There is an increase in the curvature near the touch-down point (at 486 m arc length) when the platform moves to the near position due to current forces. This increase is considerably steep for cable IAC01 with a current direction of 0°.

## 6 Array Design

For a reference farm composed of  $N_{wt}$  floating offshore wind turbines (FOWTs), its array design concerns the following aspects:

- design of the wind farm layout, i.e., the nominal positions of each FOWT, which can be denoted as  $\mathbf{L} = [x_1, x_2, \dots, x_{N_{wt}}, y_1, y_2, \dots, y_{N_{wt}}]$ , with  $[x_i, y_i]$  represents the coordinates of the  $i$ th FOWT's nominal position;
- design of mooring systems for all FOWTs, which essentially is defined by the heading angles  $\mathbf{A} = [\alpha_1, \alpha_2, \dots, \alpha_{N_{wt}}]$  of the mooring systems, since the mooring system of a FOWT assumes a symmetric setup of 3 mooring lines in this study;
- design of the inter-cable routing of the wind farm.

The array design problem is then solved by optimizing the design with respect to a chosen objective function, while respecting different realistic constraints.

A sequential approach is taken in this study, which is composed of the following steps:

- 1) optimize the wind farm layout to maximize the Annual Energy Production (AEP) of the wind farm, while respecting constraints on wind farm boundary, wind farm area, and wind turbine spacings;
- 2) optimize the heading angles of mooring systems to maximize the average clearance between anchors and avoid crossing of mooring lines;
- 3) determine the inter-cable routing to minimize the cost for the wind farm layout and mooring systems obtained in the first two steps.

### 6.1 Annual Energy Production (AEP)

To optimize the wind farm layout, we need to be able to compute the AEP of the wind farm with any potential layout. This requires the proper modelling of wind condition first. In this study, we can obtain the multi-years (2020-2022) time series of wind speed and wind direction at the hub height from the met-ocean data, which can then be used to compute the sector wise Weibull distributions and derive the joint distribution of wind speed and wind direction using the approach described in [18].

For the wind farm site, the obtained Weibull parameters and the frequency for 12 sectors are listed in Table 1-22, and the joint distribution is plotted in Figure 1-.

**Table 6-1 Sector-wise Weibull distribution parameters at hub height (150 m) at the Utsira Nord site**

$\theta_{wd}$ [deg]	0	30	60	90	120	150	180	210	240	270	300	330
$A$ [m/s]	9.13	6.59	5.82	7.89	12.09	15.63	13.04	11.31	11.44	11.41	9.87	10.73
$k$ [-]	1.96	1.97	1.85	1.85	1.98	2.43	2.40	2.10	2.00	2.07	2.05	2.09
$f$ [%]	3.39	2.88	1.96	2.76	5.74	12.17	13.78	9.54	7.97	8.41	9.08	14.25

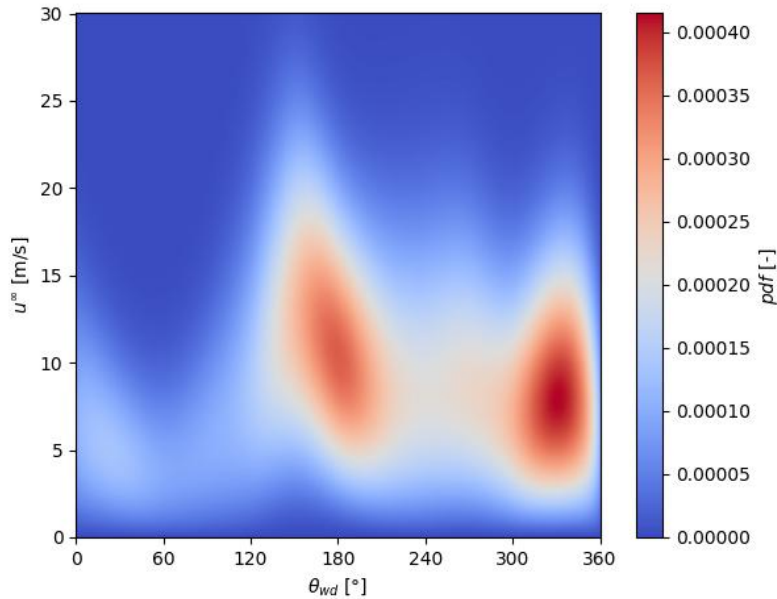


**Figure 6-13: Joint distribution of wind speed and wind direction at the wind farm site**

To compute the AEP of a FOWF (floating offshore wind farm), we meet a primary challenge caused by the movement of floating platforms, which affects wake flow and energy production. Some recent studies have begun to integrate these dynamics using high-fidelity surrogate models [19, 20]. However, these methods a database of aero-elastic simulations of FOWT under various met-ocean conditions, which can be time consuming. Also, the study by Feng et al. in [20] has shown that modelling FOWFs as bottom-fixed ones can obtain the same trend in optimization process, i.e., generating improved layout designs consistently when re-checked with simulations including impacts of platform movements, although the absolute values of AEP will see small differences. This finding demonstrated it is feasible to optimize layouts of FOWFs with engineering models that ignores the impacts of platform movements, as long as the movements are not too large.

Based on the findings in [20], we ignore the impacts brought by movements of FOWTs for the array design in this study, i.e., we compute the AEP of the FOWF in the same way as bottom-fixed wind farms.

Wind farm layout optimization commonly relies on engineering wake models for the computation of AEP, owing to their fast computational speed. While the specific procedure for AEP calculation using such models is well-documented (e.g., in [21]), we employ the open-source wind farm simulation tool PyWake [22] from DTU (Technical University of Denmark) for this purpose. PyWake provides efficient implementation of static engineering wake models, facilitating rapid AEP estimation and are extensively adopted in the field. Implementation details are available in the provided references and official documentation of the tool. In this study, the Gaussian wake model proposed by Bastankhah and Porté-Agel [23] is applied with wake expansion factor  $k=0.0325$ , and LinearSum as the wake superposition model.

## 6.2 Layout Optimization

In reality, wind turbines in a given wind farm project need to be installed inside a specific boundary, which is usually given by the energy planning authority. While the real wind farm boundaries can be very different from each other, to simplify the problem, we assume in this study that the wind farm boundary is always rectangular shape, and the layout of the turbines always takes a staggered grid layout shape. Then the whole layout of the turbines and the wind farm boundary can be

parameterized in a few variables, as shown in Figure 1-14, the blue dots represent possible locations of wind turbines, and the red dash lines represent the wind farm boundary. When the number of the possible locations is larger than the number of FOWTs, the locations closest to the center point will be removed, and the FOWTs will be placed in the remaining locations.

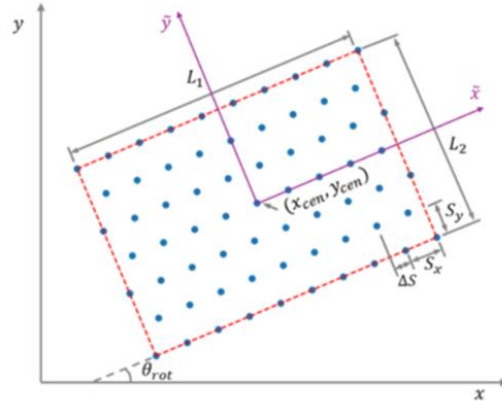


**Figure 6-14: Parameterization of a grid layout in a rectangular boundary [24]**

Based on this parameterization, and a starting grid layout, a layout optimization problem is formulated, which aims to maximize the AEP of the wind farm. The design variables will be the parameters that define the rectangular boundary and the potential turbine locations, as denoted in Figure 1-14. Constraints on the minimal spacing, i.e., the distance between any two turbines must not be below a threshold (4 rotor diameters in this study), and total wind farm area, i.e., the area of the rectangular boundary must be the same of the starting layout, are also considered. Details on the parameterization and the problem formulation can be found in [24].

Then the optimization problem is solved in this study by trying different combinations of parameters and selecting the design variables with the highest AEPs.

### 6.3 Optimization of mooring system headings

With the symmetric setup of 3 mooring lines, fixed mooring line length and fixed radius from platform to anchor, the mooring system of a given FOWT is defined by its heading angle. Then for a FOWF with a given layout, the headings can be optimized to increase the average clearance between the anchors and also avoid possible crossings of mooring lines from different FOWTs.

In this study, we compute the anchor clearance distance of a given FOWT as the minimal distance of its 3 anchors to the other turbines' anchors. Then the objective function is set as the average of all FOWTs' anchor clearance distance. The constraint considered is that any one mooring line of one FOWT should not cross any one mooring line of another FOWT. Based on this formulation, the mooring system headings of all FOWTs are optimized to maximize the average anchor clearance while respecting the non-crossing constraints. Both uniform (assuming all headings must be the same) and non-uniform (assuming all headings can be different) cases are considered and solved in a similar way.

Considering a 1 GW FOWF, which is composed of 67 FOWTs, we can first define a starting layout as a grid layout with 7 rows of turbines, with spacing between rows and columns of 7 rotor

diameters, and a 3.5 rotor diameters staggering distance. The optimization problem formulation and its solving is done using the TopDesign platform [25, 26] in this study.

Figure 1-15 shows the original layout with optimized headings, while Figure 1-16 and Figure 1-17 show the optimized layouts with 4 rows and 7 rows of FOWTs. The AEP of the layouts are also demonstrated in these figures.

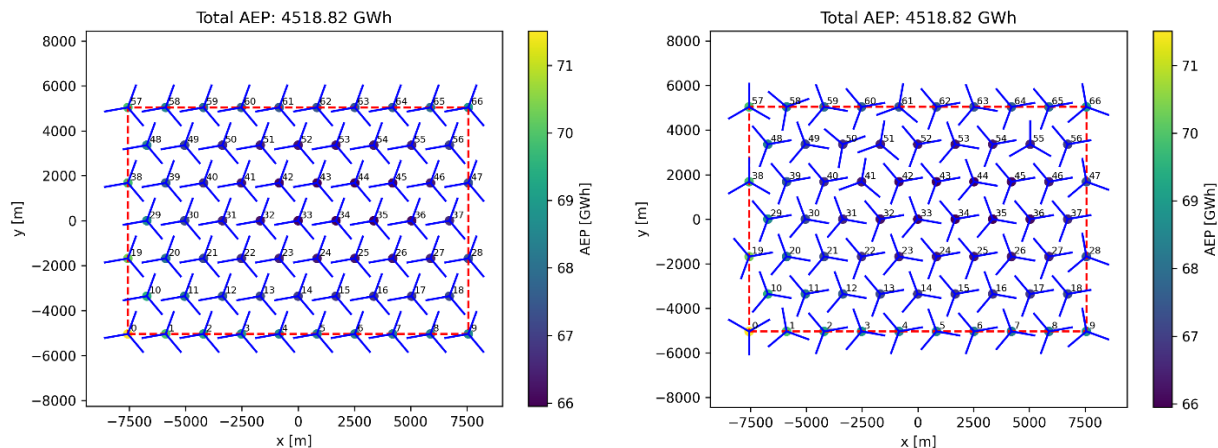


**Figure 6-15: The original layout with 7 rows of FOWTs with uniform headings (left), and nonuniform headings (right)**

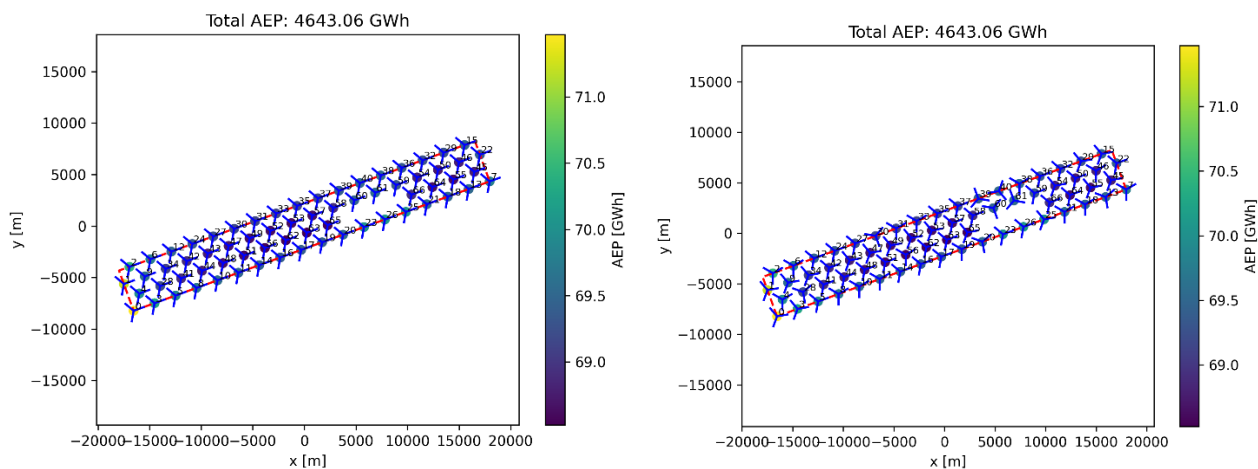


**Figure 6-16: The optimized layout with 4 rows of FOWTs with uniform headings (left), and nonuniform headings (right)**

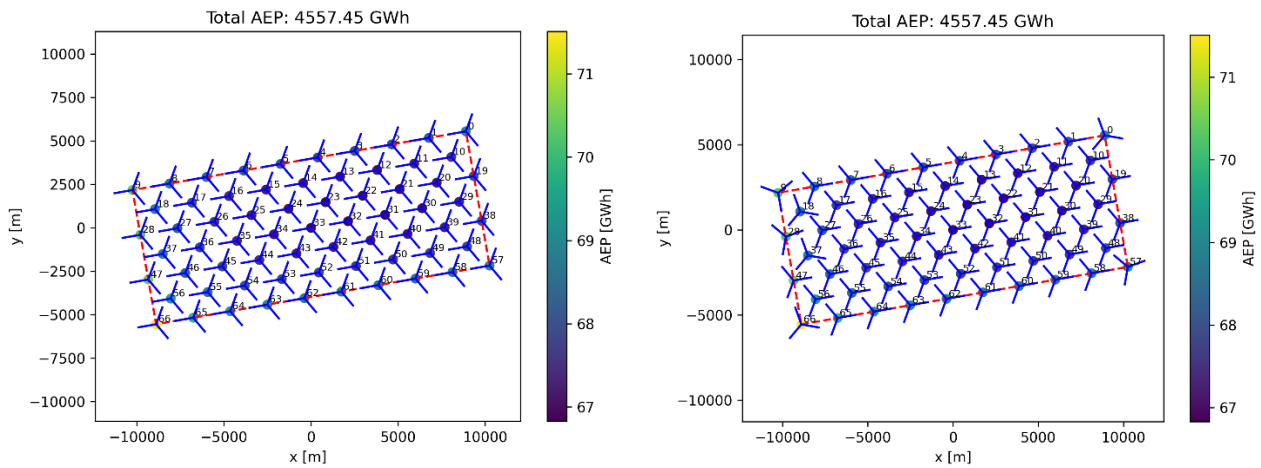


**Figure 6-17: The optimized layout with 7 rows of FOWTs with uniform headings (left), and nonuniform headings (right)**

Note that in all these layouts, while the shapes of the rectangular boundaries are different, they all have the same value of total area. Comparing the AEP values of these layout, we can also clearly see that the optimization of layout will increase the energy yield of the wind farm, and by allowing a narrower rectangular shape of the wind farm boundary, we can achieve larger AEP improvements. As the AEP of the 4 rows case increases from 4518.82 GWh to 4643.06 GWh, a 2.75% improvement, while the 7 rows case (in Figure 1-17) increases from 4518.82 GWh to 4557.45 GWh, a 0.85% improvement.

The original layout with 7 rows of FOWTs with uniform headings is taken forward for IAC and cost analysis to be used as the baseline reference farm.

## 6.4 Inter-Array Cabling (IAC)

The design of the inter-array cabling layout is linked to both the anchor configuration and the overall turbine array design. Inter-array cables connect a string of individual wind turbines to the offshore substations, enabling the collection of generated power across the wind farm. The routing of these cables must be carefully planned to achieve a balance between technical feasibility, cost efficiency, and compatibility with structural constraints.

A key consideration during design is the avoidance of anchor and mooring line interference. Each mooring occupies a defined seabed footprint that must remain clear to prevent mechanical conflict or damage during installation and operation. Cable routes between turbines are therefore planned to avoid crossing or overlapping these zones.

The IAC routing was determined following the optimisation of the WTG layout and mooring system headings described in the preceding sections. The layout described in this section is based on the original layout with uniform anchoring. The cable network connects all 67 FOWTs to a single offshore substation (OSS) located at the eastern edge of the array, at UTM31N coordinates (598059 E, 6571738 N). The OSS position was selected to minimise the total array cable length while remaining compatible with the optimised turbine layout and mooring configuration.

The 67 WTGs are arranged into seven radial strings, each originating at the OSS and terminating at the outermost turbine in the string. Four strings connect 10 WTGs and three strings connect 9 WTGs, giving the totals shown in Table 7-1. Cable routing between turbines within each string follows a centre-to-centre span length equaling 1.681 km, consistent with the turbine spacing defined in the

layout optimisation. The first cable segment in each string, connecting the OSS to the nearest WTG, varies in length depending on the relative position of the OSS to the first turbine on a given string, this distance ranges from 3.25 km to 5.78 km.

In reality the local heading of the dynamic cables should be as defined in Section 5.7, that is equally spaced between mooring lines to avoid the possibility of a clash. As an assumption, the IAC layout here assumes that the cable travels the shortest distance between WTG's, and thus neglects such. In reality a slightly increased static cable length between units would be required in order to route the dynamic cables to more favorable positions in between the moorings.

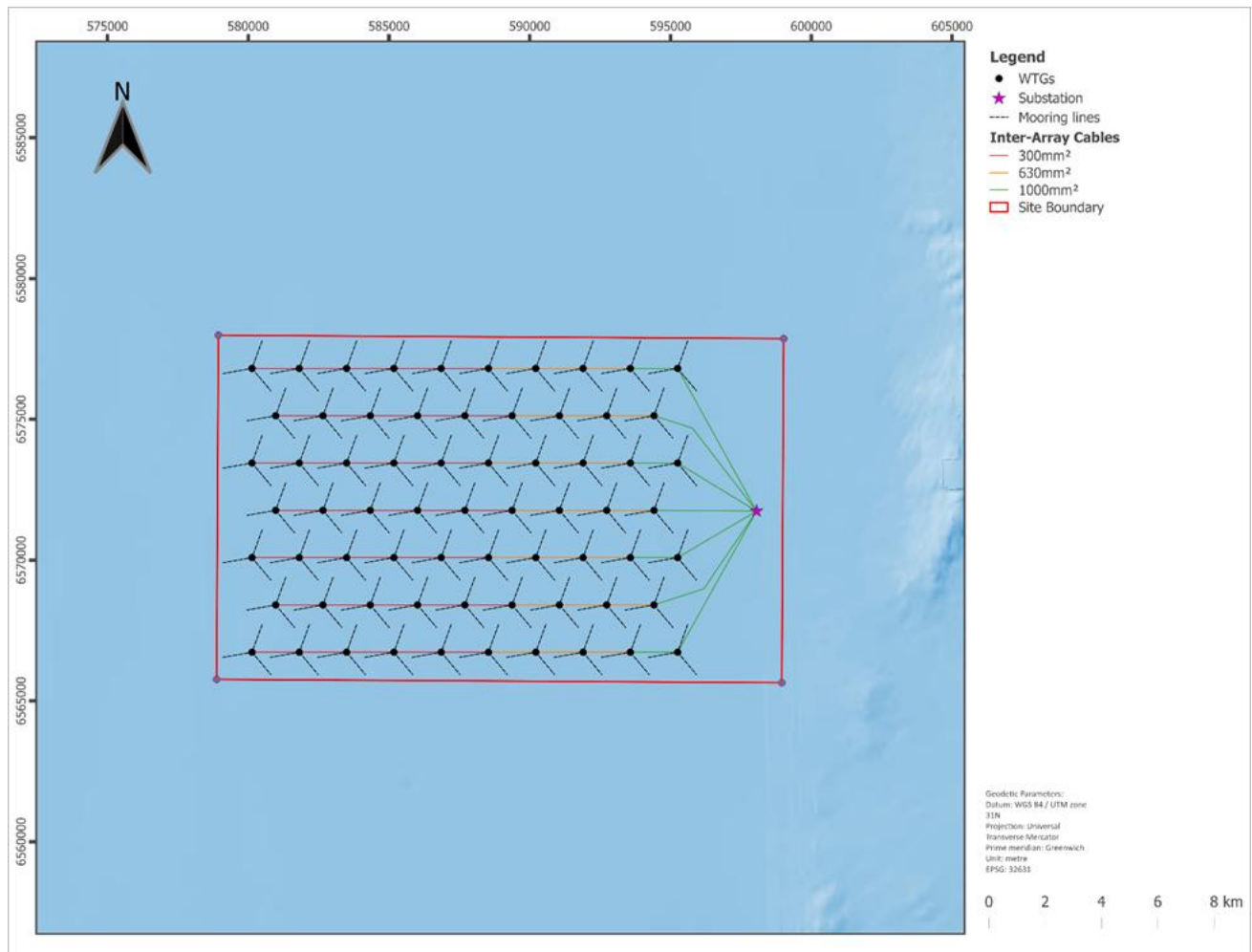


**Figure 6-1 IAC layout**

Cable conductor sizing follows a stepped approach along each string, with larger capacity caballing used at the OSS end where cumulative power flow is greatest, with progressively smaller capacity caballing towards the string tail. Three conductor sizes are used; 1,000 mm<sup>2</sup> (green), 630 mm<sup>2</sup> (orange), and 300 mm<sup>2</sup> (red). For a 10-WTG string, the first two cable segments (IAC positions 1–2) use 1,000 mm<sup>2</sup> conductors, the next three (positions 3–5) use 630 mm<sup>2</sup>, and the remaining five (positions 6–10) use 300 mm<sup>2</sup>. For a 9-WTG string, the first segment uses 1,000 mm<sup>2</sup>, the next three use 630 mm<sup>2</sup>, and the remaining five use 300 mm<sup>2</sup>. The cable sizing for each string and IAC position is summarised in Table 7-1 below.

**Table 6-2 Cable Sizing per String**

String ID	Num of WTG on string	IAC Cable Size (mm <sup>2</sup> )										
		1	2	3	4	5	6	7	8	9	10	
1	10	1000	1000	630	630	630	300	300	300	300	300	300
2	9	1000	630	630	630	300	300	300	300	300	300	NA
3	10	1000	1000	630	630	630	300	300	300	300	300	300
4	9	1000	630	630	630	300	300	300	300	300	300	NA
5	10	1000	1000	630	630	630	300	300	300	300	300	300
6	9	1000	630	630	630	300	300	300	300	300	300	NA
7	10	1000	1000	630	630	630	300	300	300	300	300	300

The total IAC network length, including both static and dynamic cables, is 159.904 km. By conductor size, this comprises 44.936 km of 1,000 mm<sup>2</sup> cable (respectively 34.244 km and 10.692 km of static and dynamic type), 43.113 km of 630 mm<sup>2</sup> cable (respectively 22.701 km and 20.412 km of static and dynamic type), and 71.855 km of 300 mm<sup>2</sup> cable (respectively 37.835 km and 34.020 km of static and dynamic type). Individual string lengths range from 20.734 km (String 4) to 24.930 km (String 1). A full summary of static cable string lengths and cable quantities by conductor size is provided in Table 6-3. As each static cable has the same dynamic cable section length on each end (0.486 km)

**Table 6-3, Cable lengths**

String ID	No. of WTG	IAC Static Cable length (km)										Total String lengths	
		1	2	3	4	5	6	7	8	9	10		
1	10	5.481	1.081	1.081	1.081	1.081	1.081	1.081	1.081	1.081	1.081	1.081	20.9
2	9	4.852	1.081	1.081	1.081	1.081	1.081	1.081	1.081	1.081	1.081	NA	18.6
3	10	2.971	1.081	1.081	1.081	1.081	1.081	1.081	1.081	1.081	1.081	1.081	18.4
4	9	3.342	1.081	1.081	1.081	1.081	1.081	1.081	1.081	1.081	1.081	NA	17.1
5	10	2.951	1.081	1.081	1.081	1.081	1.081	1.081	1.081	1.081	1.081	1.081	18.4
6	9	4.892	1.081	1.081	1.081	1.081	1.081	1.081	1.081	1.081	1.081	NA	18.6
7	10	5.431	1.081	1.081	1.081	1.081	1.081	1.081	1.081	1.081	1.081	1.081	20.9
											Total:	<b>133</b>	

**Table 6-4 Cable lengths for static and dynamic cables**

<b>String ID</b>	<b>No. of WTG</b>	<b>Total String lengths</b>	<b>Length of 1000 mm<sup>2</sup> cable</b>	<b>Length of 630 mm<sup>2</sup> cable</b>	<b>Length of 300 mm<sup>2</sup> cable</b>
<b>1</b>	10	24.93	8.506	6.159	10.265
<b>2</b>	9	22.248	5.824	6.159	10.265
<b>3</b>	10	22.42	5.996	6.159	10.265
<b>4</b>	9	20.738	4.314	6.159	10.265
<b>5</b>	10	22.4	5.976	6.159	10.265
<b>6</b>	9	22.288	5.864	6.159	10.265
<b>7</b>	10	24.88	8.456	6.159	10.265
<b>Total</b>		<b>159.904</b>	<b>44.936</b>	<b>43.113</b>	<b>71.855</b>

## 7 Conclusions

A reference floating wind array was developed by an international co-working group under the IEA Wind Task 49 “Integrated Design of Floating Wind Arrays”. This reference site is based on a generalized version of the Utsira Nord site in Norway, assuming a uniform water depth of 300 m. This reference farm is the “intermediate” water depth farm, with shallow and deep farms also developed during this project and presented in other reports.

The VolturnUS-S steel semi-submersible substructure and 15 MW WTG were used as inputs to this work.

Design load cases considering fatigue (DLC 1.2) and ultimate limit states (DLC 1.6 and DLC 6.1) were developed. Fatigue binning and an analysis of representability against the original metocean dataset has been performed.

A catenary mooring system composed of ground chain, clump weight and sheathed wire was designed and tested by ILA. Dynamic cable lazy wave configurations have been designed by using a decoupled analysis methodology.

A target capacity of 1 GW was defined considering 67 WTG units. A sensitivity study on AEP with site boundary shape was conducted, with a base case array layout presented. Optimisation of individual unit’s mooring headings was conducted to maximize spacing between anchors. Inter array cabling configuration was defined considering a single OSS.

Publicly available input files of load case tables, simulation files as well as the array ontology definition are available at the IEA Wind Task 49 GitHub<sup>1</sup> website

The reference farm presented in this report is intended to serve as base case for the floating wind research community. Further optimization and design work on the reference farm is recommended as follows: reducing the clump weight requirements, investigating the use of shared anchors, and designing dynamic cable configurations for all cable sizes as used in the IAC and cost and logistics modelling.

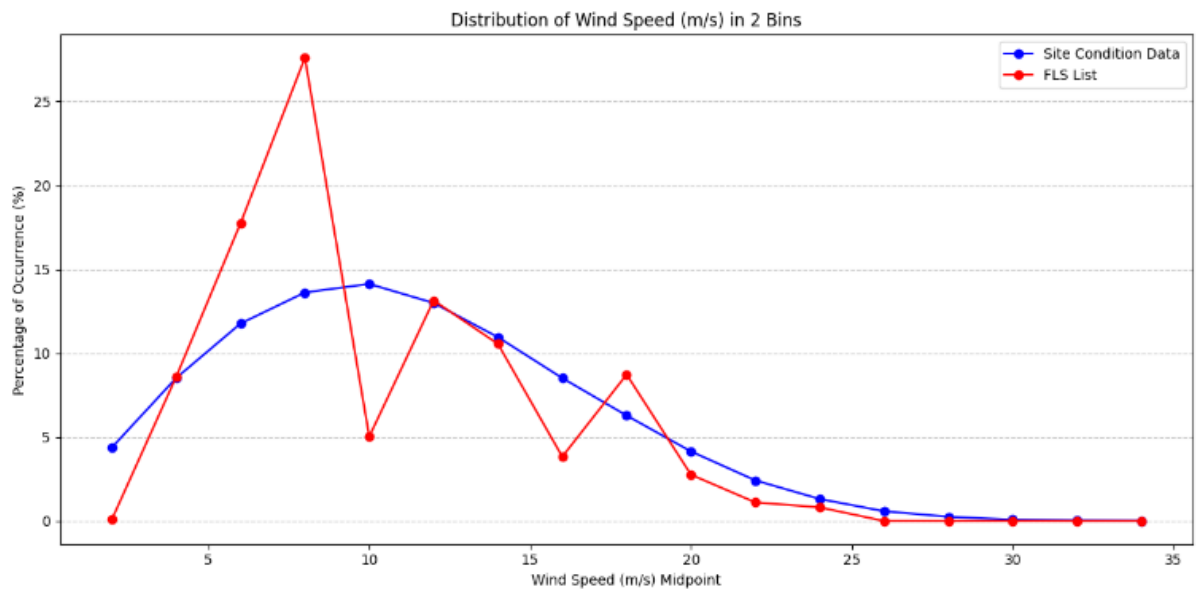
---

<sup>1</sup> [https://github.com/IEAWindTask49/Reference\\_Array\\_Intermediate](https://github.com/IEAWindTask49/Reference_Array_Intermediate)

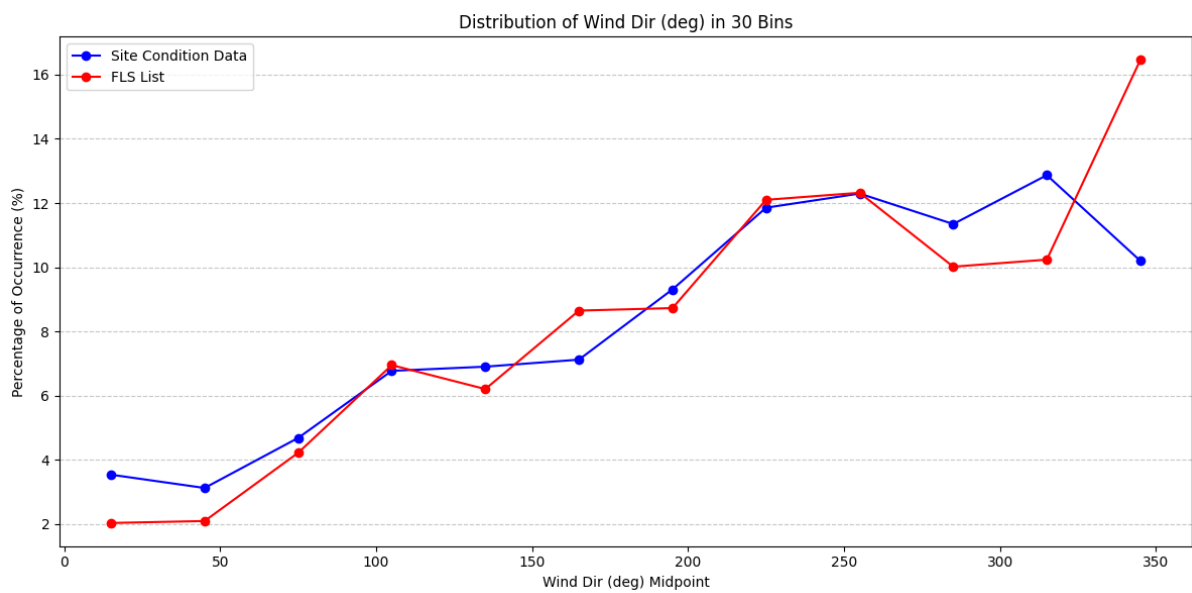
## References

- (API), A. P. (2005). *Design and Analysis of Stationkeeping Systems for Floating Structures*.
- Allen, C., Viscelli, A., Dagher, H., Goupee, A., Gaertner, E., Abbas, N., . . . Barter, G. (2020). *Definition of the UMaine VoltturnUS-S reference platform developed for the IEA wind 15-megawatt offshore reference wind turbine*. No. NREL/TP-5000-76773.
- American Bureau of Shipping (ABS). (2013). *Offshore Anchor Data for Preliminary Design of Anchors of Floating Offshore Wind Turbines*. Houston, Texas: American Bureau of Shipping (ABS).
- Author. (xxxx). Title. *Journal Name*, x(x), x-x.
- B. J. Jonkman. (2016). *TurbSim*. (NREL) Retrieved from <https://www2.nrel.gov/wind/nwtc/turbsim>
- Cheyne, E., Li, L., & Z., J. (2024). Metocean conditions at two Norwegian sites for development of offshore wind farms. *Renewable Energy, Volume 224*.  
doi:<https://doi.org/10.1016/j.renene.2024.120184>
- Creane, S. P.-P. (2024). *Reference Site Conditions for Floating Wind Arrays*. . Golden, CO: National Renewable Energy Laboratory. NREL/TP-5000-89937. <https://docs.nrel.gov/docs/fy24ost>.
- Devantier, C. B., Wong, X. H., & Schrameyer, V. (2024, April). Marine growth along the mesopelagic zone. Retrieved June 09, 2025, from <https://zenodo.org/records/12731585>
- DNV. (2021). *Recommended Practice Environmental Conditions and Environmental Loads DNV RP C205*.
- DNV. (July 2021). *Position Mooring DNV-OS-E301*. DNV.
- Gaertner, E., Rinker, J., Sethuraman, L., Zahle, F., Anderson, B., Barter, G., . . . Skrzypinski, W. (2020). *Definition of the IEA 15-Megawatt Offshore Reference Wind Turbine*.
- Hall, M., Lozon, E., McAuliffe, F. D., Bessone, M. B., Bayati, I., Bowie, M., . . . Reddy, M. (June 2024). *The IEA Wind Task 49 Reference Floating Wind Array Design Basis*. NREL/TP-5000-89709.
- IEC. (2019). *IEC 61400-3-1 Wind energy generation systems – Part 3-1: Design requirements for fixed offshore wind turbines*.
- Institute, N. M. (n.d.). *NORA3 3-km Norwegian Reanalysis*. Retrieved from <https://thredds.met.no/thredds/projects/nora3.html>
- Kanner, S., Aubault, A., Peiffer, A., & Yu, B. (2018). Maximum Dissimilarity-Based Algorithm for Discretisation of Metocean Data Into Clusters of Arbitrary Size and Dimension. *ASME 2018 37th International Conference on Ocean, Offshore and Arctic Engineering*.  
doi:10.1115/OMAE2018-77977
- Orcina Ltd. (n.d.). *OrcaFlex Examples: K03 15MW semi-sub FOWT*. Retrieved from <https://www.orcina.com/resources/examples/?key=k#39>
- Rezaeifar, M. (2025). *IDEA-IRL WP1-D1F: Reference Site Technical Report: Ground Conditions Summary*.
- Vertias, B. (July 2021). *Classification of Mooring Systems for permanent and Mobile Offshore Units. NR 493 DT R04 E*. Paris.
- Wright, C., Friel, D., Vatandoust, A. R., Tavangar, S., McAteer, J., Almoghayer, M. A., . . . Bohan, G. (2026). *IDEA-IRL- WP2-D2: Definition of the IDEA-IRL Reference Floating Wind Farm Designs*. Draft.

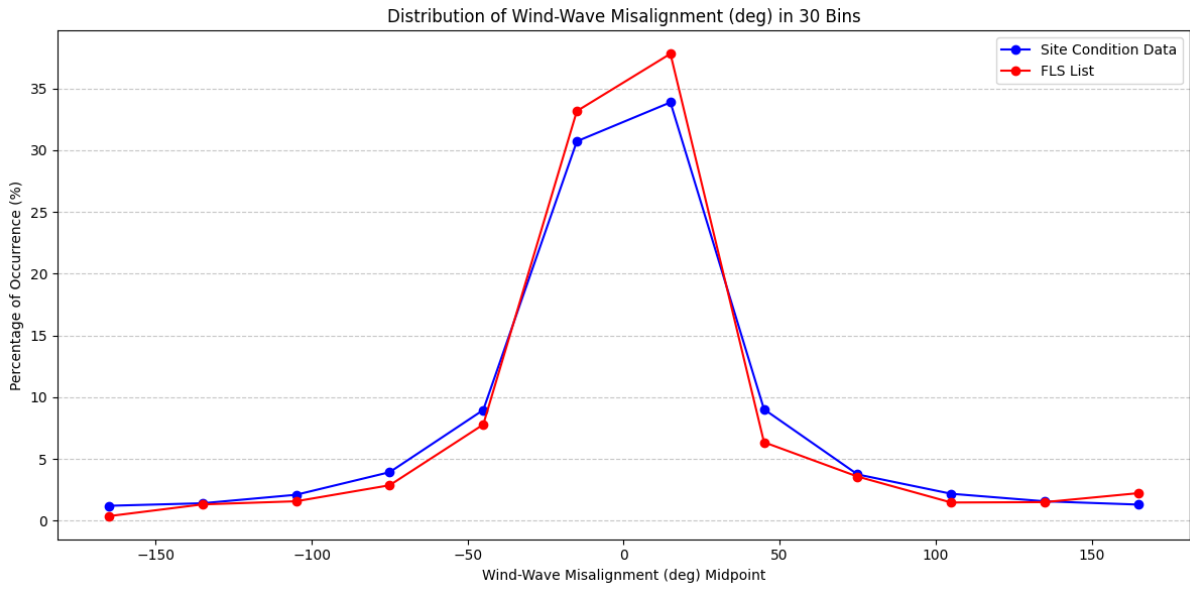
## Appendix A. Fatigue Binning Representability



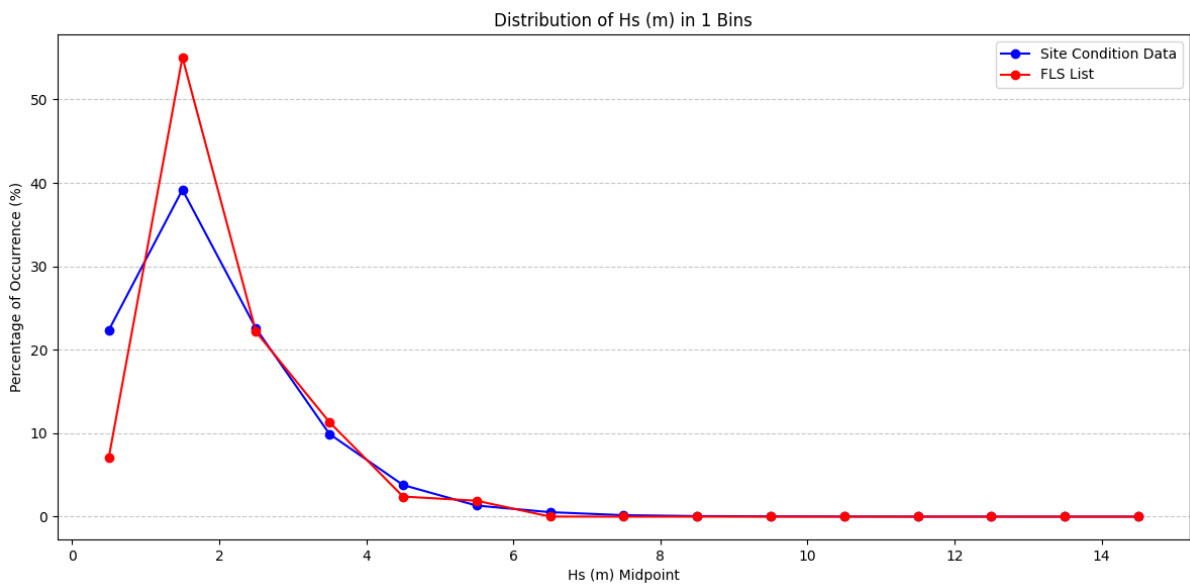
**A- 1: Percentage occurrences of wind speed, comparing site conditions against selected fatigue cases**



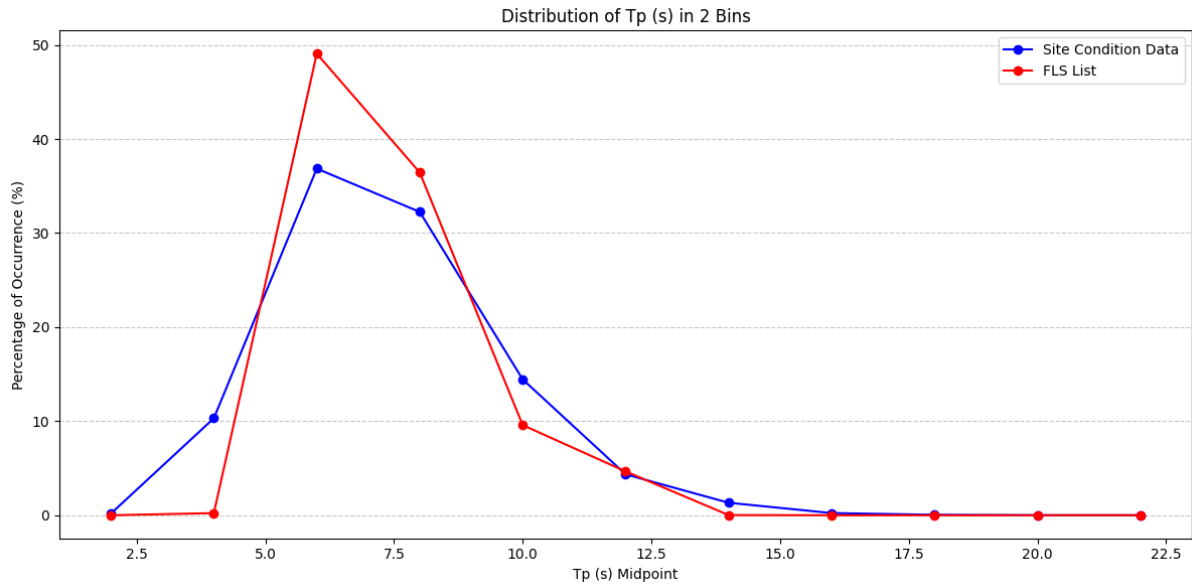
**A- 2: Percentage occurrences of wind direction, comparing site conditions against selected fatigue cases**



**A- 3: Percentage occurrences of wind-wave misalignment, comparing site conditions against selected fatigue cases**

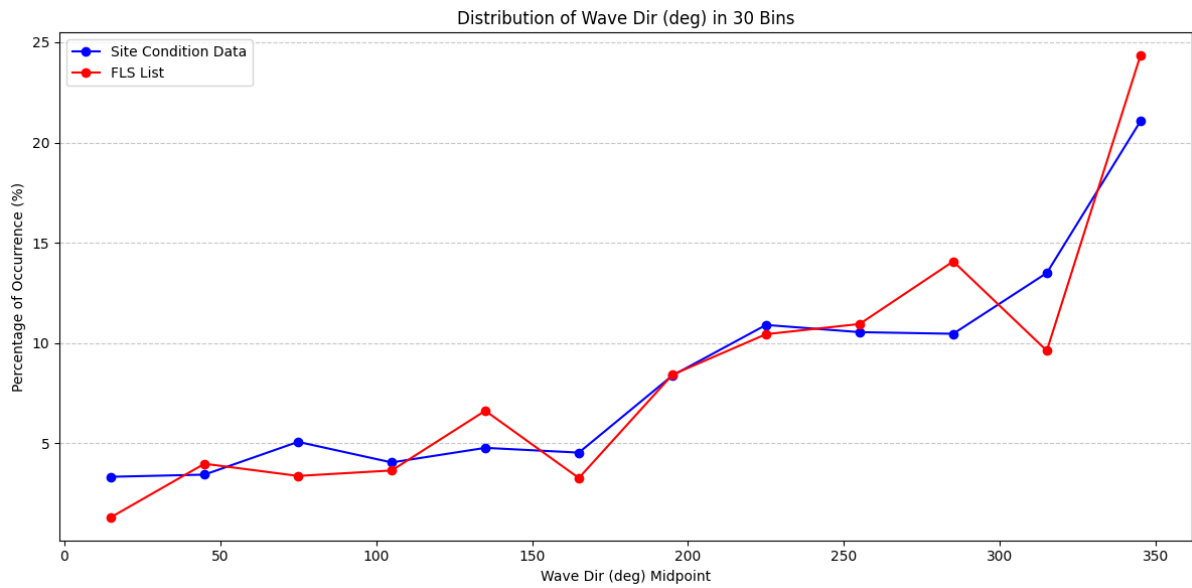


**A- 4: Percentage occurrences of significant wave height, comparing site conditions against selected fatigue cases**

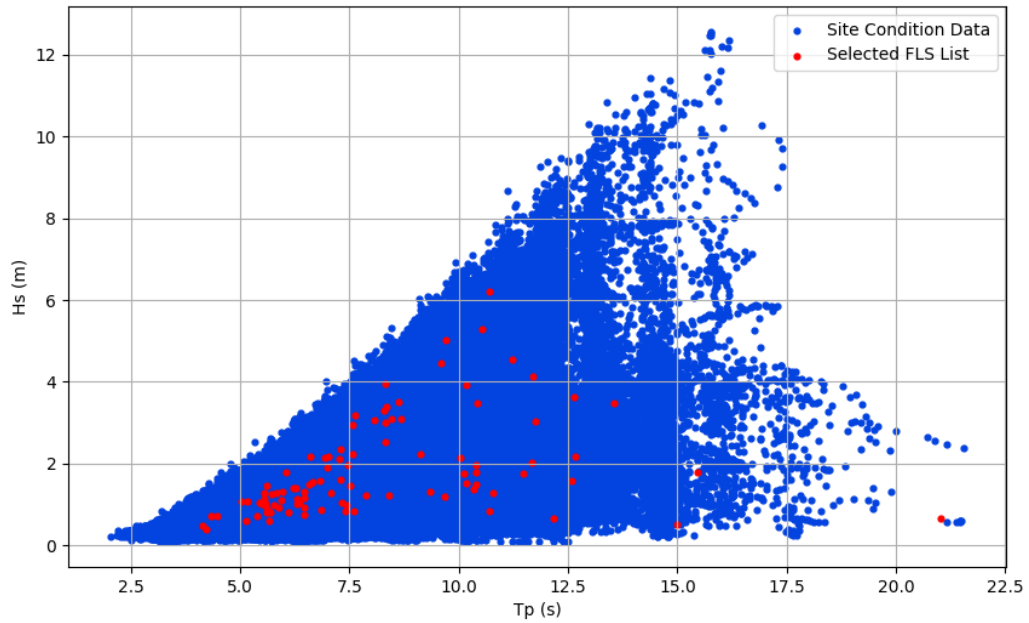


**A- 5: Percentage occurrences of wave peak period, comparing site conditions against selected fatigue cases**

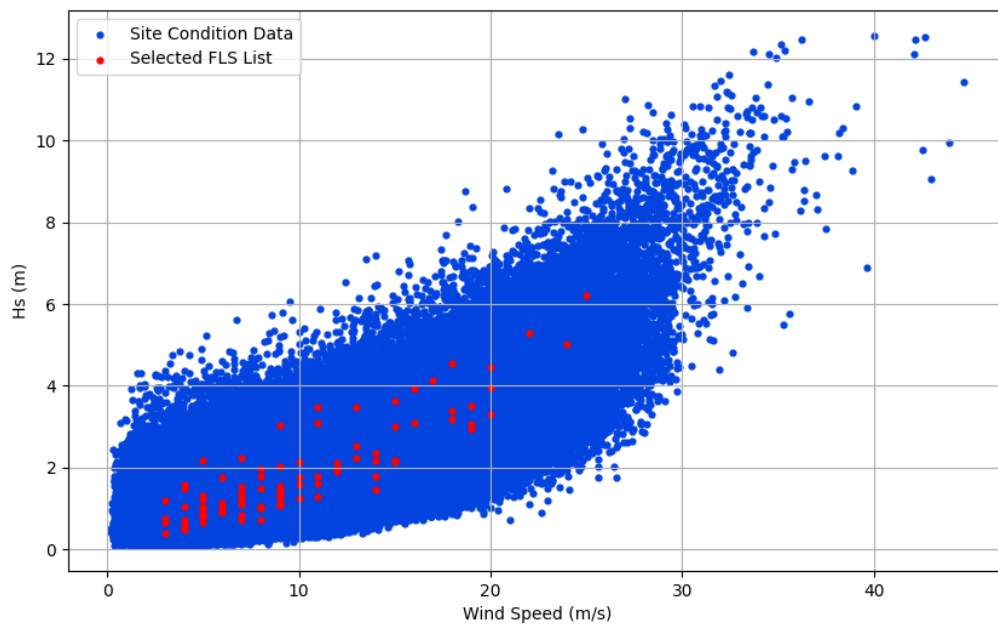
(f)



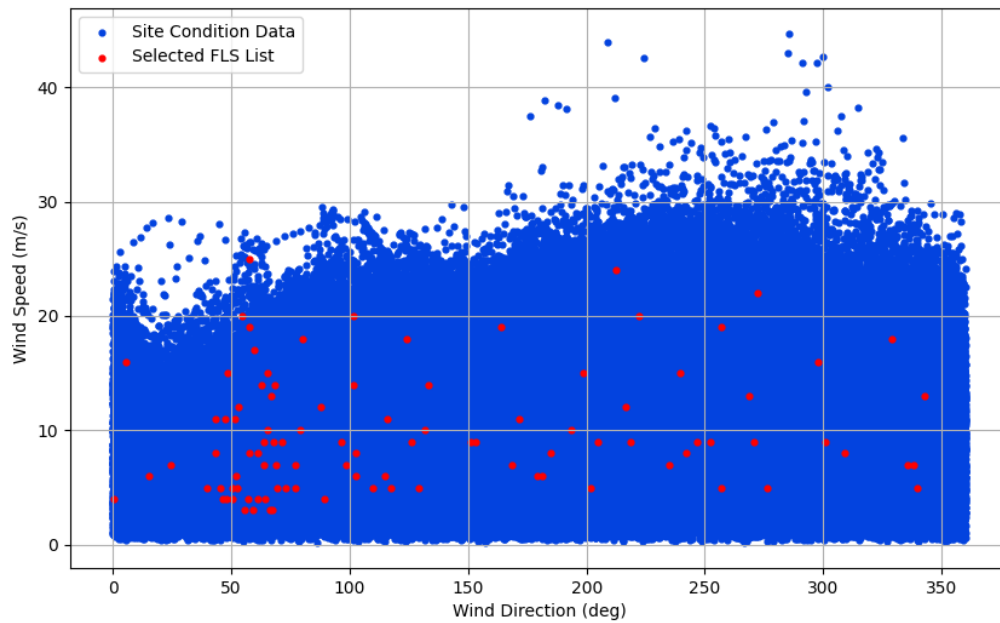
**A- 6: Percentage occurrences of wave direction, comparing site conditions against selected fatigue cases**



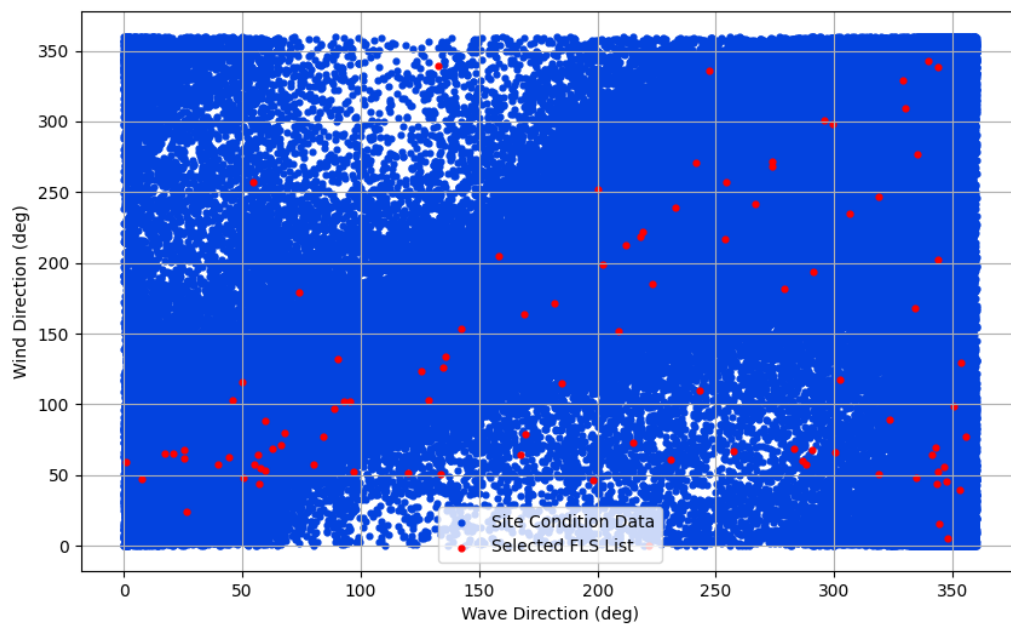
**A- 7: Significant Wave Height vs Peak Period ( $H_s/T_p$ ) Scatter plot for Site data and selected FLS List data**



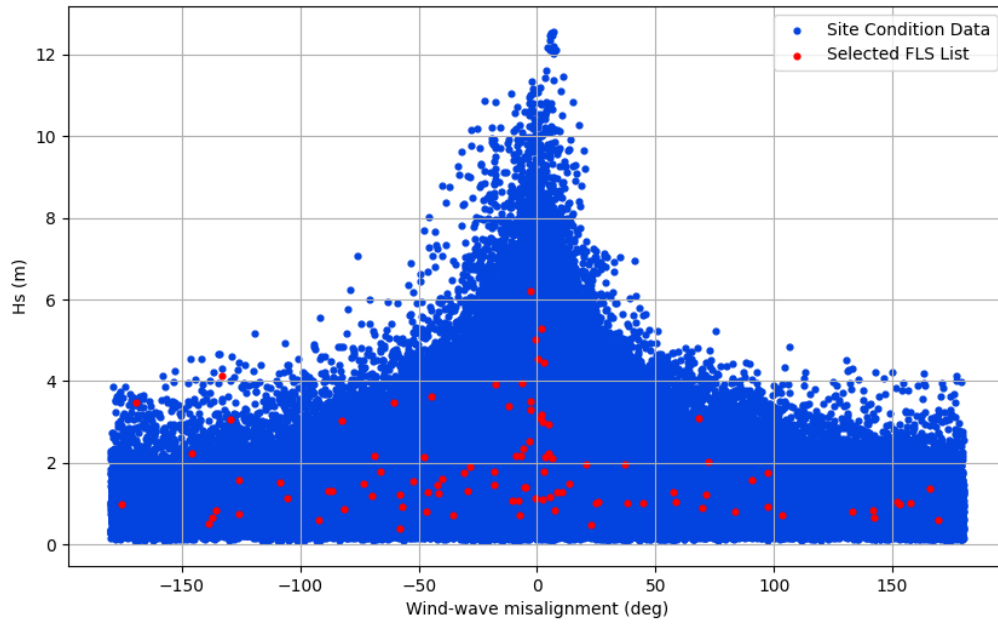
**A- 8: Significant Wave Height vs Wind Speed scatter plot for site data and selected FLS List data**



**A- 9: Wind Speed vs Wind Direction Scatter plot for Site data and selected FLS List data**



**A- 10: Wind Direction vs Wave Direction Scatter plot for Site data and Selected FLS List data**



**A- 11: Significant Wave Height (Hs) vs Wind-wave Misalignment Scatter plot for Site data and Selected FLS List data:**